Immobilization and One-Dimensional Arrangement of Virus Capsids With Nanoscale Precision Using DNA Origami

Nicholas Stephanopoulos‡[1], Minghui Liu‡[2], Gary J. Tong[1], Zhe Li[2], Yan Liu[2], Hao Yan*[2], and Matthew B. Francis*[1]

[1]Department of Chemistry, University of California, Berkeley, and Materials Sciences Division, Lawrence Berkeley National Labs, Berkeley, California 94720-1460. [2]Department of Chemistry and Biochemistry and the Biodesign Institute, Arizona State University, Tempe AZ 85287

Supporting Information

General: Unless otherwise noted, all chemicals and solvents were of analytical grade and were used as received from commercial sources. Water (ddH_2O) used in biological procedures or as reaction solvents was deionized using a NANOpure purification system (Barnstead, USA). The centrifugations required in spin-concentration steps were conducted using a Sorvall Legend Mach 1.6R centrifuge (Thermo Fisher Scientific, USA).

Prior to analysis, biological samples were desalted and separated from small molecule contaminants using NAP-5 or NAP-10 gel filtration columns (Amersham Biosciences, USA). MS2 capsids elute in the void volume of these columns, while small molecules are retained. Additionally, 100,000 Da molecular weight cut-off filters (Millipore, USA) were employed as indicated below.

All oligonucleotides were obtained from Integrated DNA Technologies (www.idtdna.com). The origami staple strands were ordered in the format of 96-well plates that were normalized to 100μM, and were used without further purification. The probe strands were purified by denaturing PAGE. Then concentration of each strand was measured and estimated by measuring the OD260 (Eppendorf, USA). Oligonucleotides for capsid conjugation were purified by reverse-phase HPLC or NAP-5 gel filtration columns (GE Healthcare). Samples were lyophilized using a LAB CONCO Freezone 4.5 (Lab Conco). Lyophilized oligonucleotides were re-suspended in the appropriate buffer and the concentration was determined by measuring the OD260.

UV-Vis: UV-Vis spectroscopic measurements were conducted on a Cary 50 Scan benchtop spectrophotometer (Varian Inc., USA).

Protein gel analysis: For protein analysis, sodium dodecyl sulfate-polyacrylamide gel electrophoresis (SDS-PAGE) was accomplished on a Mini-Protean apparatus (BioRad, USA), following the general protocol of Laemmli.[1] Commercially-available markers (BioRad, USA) were applied to at least one lane of each gel for calculation of apparent molecular weights. Visualization of protein bands was accomplished by staining with Coomassie Brilliant Blue R-250 (BioRad, USA). Gel imaging was performed on an EpiChem3 Darkroom system (UVP, USA).

Transmission Electron Microscopy (TEM): The TEM images in Figures 2D and S24, the top two images in Figure S25, and the last eight images in Figure S26 were prepared for TEM analysis by applying analyte solution to carbon-coated copper grids (400 mesh, Ted Pella, USA) for 3 min, followed by rinsing with ddH2O. The grids were then exposed to a solution of uranyl acetate (15 mg/mL in ddH_2O) for 90 seconds as a negative stain and rinsed with ddH_2O. TEM images were obtained at the Berkeley Electron Microscope Lab using a FEI Tecnai 12 transmission electron microscope with 120 kV accelerating voltage.

The TEM images in Figure 2C, the bottom two images in Figure S25, and the first five images in Figure S26 were prepared by applying the sample solution (2.5 μL) onto carbon-coated grids (400 mesh, Ted Pella, USA). Before depositing the sample, the grids were glow discharged using an Emitech K100X machine. After deposition, the sample was wicked from the grid with a piece of filter paper. The grid was

washed with water by touching it quickly with a drop of water and wicking away the excess using filter paper. The origami-capsid complex sample was stained using 0.7% uranyl formate and imaged using a Philips CM12 transmission electron microscope, operated at 80kV in the bright field mode.

For Tri3 tiles, the capsids were clearly visualized as hollow spherical structures (Figures 2D, S24); for Tri1 tiles, however, the capsids did not stain as well, and the walls are not as easily discerned in some cases (Figures 2C, S23). The size of these objects (~30 nm) and the fact that in some of them the walls can be distinguished makes us confident that these are indeed the capsids. For arrays formed with rectangular tiles and capsids (either using M or DC tiles; Figures S25 and S26, respectively), the arrays adsorb to the grid edge-on, so the tile is visualized as a line connecting the capsids. The inter-capsid aggregation on the surface (which is commonly observed with MS2) often prevented distinguishing individual arrays as by AFM, but in numerous cases individual capsids clearly linked by tiles are visible. We note that the tiles are flexible and can curve, as seen in the TEM images, unlike in the AFM images where they adsorb flat on the surface.

Atomic Force Miscroscopy (AFM): After annealing samples, the tile-capsid conjugates were analyzed by tapping-mode AFM. To prepare samples, first 2 μL of 1 mM $NiCl_2$ in ddH_2O was applied to a freshly cleaved mica surface for 2 min. Next, 2 μL of sample was applied for an additional 2 min. The mica was then rinsed by dipping into ddH2O and dried using a stream of nitrogen. Images were obtained using a Veeco Nanoscope V scanning probe miscroscopy (Veeco, USA) using FM-50 tips with a 75 kHz resonant frequency and a force constant of 2.8 N/m (Nano World, USA).

The AFM images in Figures S3 and S9 were performed under 1x TAE-Mg^{2+} buffer (40 mM Tris, 20 mM acetic acid, 2 mM EDTA, 12.5 mM $Mg(OAc)_2$, pH 8.0) in a fluid cell in tapping mode, using the tip on the shorter cantilever of the SNL tips (Veeco, USA). The sample (2 μL) was first deposited onto the freshly cleaved mica surface and left to adsorb for 1min. Then, 35 μL of 1x TAE-Mg^{2+} buffer was added onto the surface before obtaining the image.

Design of origami tiles: The position of each probe strand was determined using the software program Tiamat (developed by the Yan Lab and collaborators: http://yanlab.asu.edu/Resources.html). The design of the rectangular origami tiles was as shown in Figure S1.The design of triangular origami was used as previously described by Rothemund, and as shown in Figure S2.[2] A polyA/T hybridization strategy was chosen over a polyG/C strategy to avoid potential problems due to G-quadruplex formation.

Formation of single origami tiles: The origami tiles were formed according to the method of Rothemund.[2] A molar ratio of 1:5 between the long M13 viral ssDNA and the short unmodified staple strands was used. The probe strands for hybridization with the poly-T strands on the capsid were used in 10:1 ratio to that of the viral DNA. Origami tiles were assembled in 1x TAE-Mg^{2+} buffer (40 mM Tris, 20 mM acetic acid, 2 mM EDTA, 12.5 mM $Mg(OAc)_2$, pH 8.0) by cooling slowly from 90 °C to room temperature. The origami tiles and excess staples were then separated by EtBr stained 1.5% agarose gel (running buffer 1x TAE-Mg^{2+} buffer, 10 V/cm), running in an ice-water bath. The band corresponding to the tiles was excised and the probe tiles were extracted from the gel using Freeze N' Squeeze columns (Bio-Rad, USA). After purification, the tiles were then concentrated using 100 kDa Microcon centrifugal filter devices (Millipore, USA). The final concentration of origami tiles was estimated according to the dsDNA absorbance at 260nm and the calculated extinction coefficient (http://biophysics.idtdna.com/).

Single tile analysis: Purified origami tiles were verified by both EtBr stained 1.5% agarose gel (the same as the purification step) and AFM (Figure S3). Samples (10 μL) were mixed with 1 μL 10x native gel loading dye and then loaded into each well.

Production of N87C T19paF MS2: The unnatural amino acid p-aminophenylalanine (*p*aF) was

incorporated into MS2 as previously described.[3] The N87C/T19*p*aF mutant plasmid was created by site-directed mutagenesis of the pBAD-T19*p*aF MS2 vector using forward primer following the Qiagen protocol:

5'-AGCCGCATGGCGTTCGTACTTATGTATGGAACTAACCATTC-3'

and reverse primer:

5'-GAATGGTTAGTTCCATACATAAGTACGAACGCCATGCGGCT-3'.

The pBAD-N87C/T19*p*aF was subsequently grown and purified as previously described.[3]

Modification of MS2 with Oregon Green (OG) maleimide: The modification of capsids with OG maleimide was carried out as previously described.[4] To a solution of N87C T19*p*aF MS2 (80 μM in 10 mM phosphate buffer, pH 7) was added 20 equivalents of Oregon Green maleimide as a 100 mM solution in DMF. The reaction mixture was vortexed briefly, and then incubated at RT for 2 h in the dark. The mixture was then passed through a NAP-5 column equilibrated with 10 mM phosphate buffer, pH 7, to remove excess chromophore. The capsids were further concentrated using a 100,000 Da molecular weight cut-off filter. The conversion of porphyrin was determined by comparing the absorbance of the Oregon Green absorption maximum (ε = 80,000 $M^{-1}cm^{-1}$) to the A260 of the protein (ε = 172,000 $M^{-1}cm^{-1}$) and assuming negligible dye absorbance at 260 nm. All exctinction coefficients were determined in 10 mM phosphate, pH 7, the buffer in which the MS2 conjugates were stored.

DNA attachment via oxidative coupling: The $(T)_{20}$ ssDNA sequence was appended to MS2 capsids modified inside with Oregon Green (OG) as previously described.[5] To synthesize the phenylene diamine conjugate necessary for the oxidative coupling, DNA strands containing a primary amine at the 5'-end were reacted with 4-(4-diethylamino-phenylcarbamoyl)-butyric acid (60-120 eq.) in a 1:1 solution of DMF and 50 mM phosphate buffer, pH 8. The reaction mixture was allowed to react at RT for 2 h, then purified by gel filtration to remove excess small molecule. The DNA was then lyophilized and resuspended in the desired buffer. The concentration was determined by measuring the absorbance at 260 nm.

The phenylene diamine-modified DNA strand was next attached to the MS2-OG conjugate via the oxidative coupling reaction as previously described. An Eppendorf tube was charged with MS2-OG (20 μM), the phenylene diamine-modified oligonucleotide (200 μM), and $NaIO_4$ (5 mM). The reaction mixture was vortexed and allowed to react at RT for 1 h. The reaction was quenched by the addition of 1/10 volume of 500 mM TCEP, then purified by NAP-5 filtration and spin-concentration using 100 kDa molecular weight cut-off filters.

Procedure for annealing of capsids to tiles: For annealing reactions between capsids and tiles, the components were mixed in 2x TAE-Mg^{2+} buffer (80 mM Tris, 40 mM acetic acid, 4 mM EDTA, 25 mM $Mg(OAc)_2$, pH 8.0) and annealed from 37 to 4 °C at a rate of 1 °C/min on a S1000 Thermal Cycler PCR machine (Bio-Rad, USA). Typical final tile concentration was ~2 nM, and the capsid concentration was scaled accordingly (e.g. ~ 4 nM in capsid for the experiments described in the paper). To make the E and M tile arrays, a small aliquot (~1 μL) of a concentrated solution of linker strands was added (either 5 or 10 equivalents) to the mixture prior to annealing. For the DC tile arrays, 5 equivalents of the edge staples (again as a small aliquot of concentrated solution) were added to the mixture prior to annealing. All samples were imaged by AFM immediately following annealing in order to prevent inter-tile or inter-array aggregation with time. A 2x concentration of buffer was used because we found that it gave longer arrays in general, most likely due to the increased electrostatic screening of the higher-salt buffer.

It appears that origami tiles and DNA in general bind to the mica surface with a greater efficiency

than the MS2-dye-DNA conjugate or capsids alone. Thus, the two-fold excess of capsids used in most experiments is not obvious from inspecting the AFM images alone. Furthermore, in Figure S19, almost no capsids can be seen in the AFM image despite a two-fold excess relative to tiles. This is likely due to the large excess of $(T)_{40}$ ssDNA added, which preferentially binds the mica and passivates it against capsid binding.

Virtually 100% efficiency of capsid-tile association was also observed upon incubating the components at 4 °C overnight (without an annealing step), but we used the annealing procedure due to the efficacy and speed it afforded. We have also observed that prolonged incubation of capsids and tiles results in lower-quality images for as of yet undetermined reasons, so shorter incubation times were preferred.

The dye modification of the interior of the capsids with OG did not have any effect on the hybridization efficiency. Capsids that did not contain the dye associated just as effectively with the tiles as capsids with the dye.

An "on-surface" association of tiles with capsids was also attempted. In this experiment, we took tile arrays formed without MS2 and deposited them on the surface first. After rinsing and drying the mica surface, a dilute solution of DNA-modified capsids was applied for about 5 minutes. Imaging by AFM showed that while a modest fraction of binding sites on the tiles contained MS2, there was too much non-specific background adsorption of capsids to the surface to make this approach useful. Furthermore, this approach may not be optimal because the arrays could bind to the surface with the probe strands facing downward, preventing access by the ssDNA on the capsids.

Array length distribution quantification: To determine the distribution of array lengths shown in Figures S20-S22, multiple AFM images were obtained for each sample calculated (not all images were included in the Supporting Information). Manual counting of these images yielded the statistics reported in the distributions. For single tiles, visual inspection determined whether a tile had a capsid or not, and whether more than one tile was bound to a given capsid. Broken or incompletely formed tiles were not counted.

In counting the E and M tile arrays, only arrays that were completely in the field of view of the AFM image were counted. Furthermore, only arrays that were clearly distinguishable were counted; occasional aggregates that prevented distinguishing individual arrays were disregarded. Array lengths are reported based on the number of tiles in an array; however, the association efficiency of tiles with capsids remained close to 100%, so the tile array length correlates pretty much exactly with the capsid array length.

In counting the DC tile arrays, once again only arrays that were completely in the field of view were counted, and large aggregates were disregarded. Due to the presence of tile edges without capsids bound, array lengths were reported with respect to the number of capsids in a row. The total number of tile edges without capsids was determined, as well as the number of branch points (defined as capsids that had more than two tiles bound to them).

Control experiments: Control experiments were first carried out using the three rectangular tiles (E, M, and DC) and capsids modified with the dye but not with DNA (Figures S15-S17). Edge staples were added in the mixture as well for the case of the DC tiles. No significant association of the capsids with the tiles was observed; in addition, the DC tiles show significant edge stacking due to the staples added, indicating that this factor was an important "pre-organization" effect that aided the array result in Figure 3D. Control experiments were also carried out with E tiles bearing a random 40-nt sequence and capsids modified with the $(T)_{20}$ sequence used in the main experiments (Figure S18). Once again, no significant association of the capsids with the tiles was seen.

In another experiment, MS2-OG-$(T)_{20}$ was mixed with E tiles (bearing the correct $(A)_{40}$ sequence) and annealed, then in a second step a large excess (~1000-fold) of $(T)_{40}$ ssDNA was added and a second annealing carried out. The competing strand binds to the 40-nt probe on the tiles with a greater affinity than the 20-nt strands on the MS2; combined with the large excess added, this effect results in the displacement

of the MS2 strands from the tile (Figure S19). Fewer tiles are seen on the surface than in other experiments, likely due to the passivation of the surface to MS2 binding due to the excess $(T)_{40}$ strand. The removal of the MS2 upon addition of the $(T)_{40}$ strand not only confirms the DNA-specific binding of the capsids, but also suggests a possible way to remove the capsids from the tiles if capsid release is required at a later time.

E tile probe sequences:

Probe-57:
AACAGGGAAGCGCAGAACAAAGTCAGAGGGTAATTGAGCGCTTATTACGCA
GTATGAAAAAAAAAAAAAAAAAAAAAAAAAAAAAAAAAAAAA

Probe-82:
AGTAATTCTGTCCACGAGCCAGTAATAAGAGAATATAAAGTAATCCAATCGC AAGAAAAAA
AAAAAAAAAAAAAAAAAAAAAAAAAAAAAAAAA

Probe-107:
TAATGCAGAACGCGATATTTAACAACGCCAACATGTAATTTAATATTTTAGTT
AATAAAAAAAAAAAAAAAAAAAAAAAAAAAAAAAAAAAAAA

M tile probe sequences:

Probe-85:
GAAGGAGCGGAATTGTTTGAGTAACATTATCATTTTGCGGAATGCAACAGTG
CCACAAAAAAAAAAAAAAAAAAAAAAAAAAAAAAAAAAAAAA

Probe-87:
GCTGAGAGCCAGCAAGGTGAGGCGGTCAGTATTAACACCGCCCCAGCCATTG
CAACAAAAAAAAAAAAAAAAAAAAAAAAAAAAAAAAAAAAA

Probe-89:
AGGAAAAACGCTCAGCTGGTAATATCCAGAACAATATTACCGCGCGCTTAAT
GCGCAAAAAAAAAAAAAAAAAAAAAAAAAAAAAAAAAAAAA

Probe-110:
GGCAATTCATCAATACTCGTATTAAATCCTTTGCCCGAACGTTAAAGCATCAC
CTTAAAAAAAAAAAAAAAAAAAAAAAAAAAAAAAAAAAAAA

Probe-112:
GCTGAACCTCAAATCATTAAAAATACCGAACGAACCACCAGCTTTTGACGCT
CAATAAAAAAAAAAAAAAAAAAAAAAAAAAAAAAAAAAAAA

Probe-114:
CGTCTGAAATGGATAACATCACTTGCCTGAGTAGAAGAACTCTGACGAGCAC
GTATAAAAAAAAAAAAAAAAAAAAAAAAAAAAAAAAAAAAA

DC tile probe sequences:

Probe-17:
TATCACCGTCACCGCCATCTTTTCATAATCAAAATCACCGGATCAGAGCCGCC
ACCAAAAAAAAAAAAAAAAAAAAAAAAAAAAAAAAAAAAAA

Probe-18:
CTCAGAACCGCCACAGGAGTGTACTGGTAATAAGTTTTAACGTATAAACAGT
TAATAAAAAAAAAAAAAAAAAAAAAAAAAAAAAAAAAAAAA

Probe-19:
GCCCCCTGCCTATTGAACCGCCACCCTCAGAGCCACCACCCTAACCCATGTAC
CGTAAAAAAAAAAAAAAAAAAAAAAAAAAAAAAAAAAAAAA

Probe-20:
AACACTGAGTTTCGTCACGTTGAAAATCTCCAAAAAAAAAGGCTTATCAGCTT
GCTTAAAAAAAAAAAAAAAAAAAAAAAAAAAAAAAAAAAAA

Probe-21:
TCGAGGTGAATTTCTGAGGAAGTTTCCATTAAACGGGTAAAACTAAAACGAA
AGAGAAAAAAAAAAAAAAAAAAAAAAAAAAAAAAAAAAAAA

Probe-152:
CGCTATTAATTAATAATAAAGAAATTGCGTAGATTTTCAGGTTATCAAAATTA
TTTAAAAAAAAAAAAAAAAAAAAAAAAAAAAAAAAAAAAAA

Probe-160:
GCACGTAAAACAGAGCACTAACAACTAATAGATTAGAGCCGTAGGAAGGTT
ATCTAAAAAAAAAAAAAAAAAAAAAAAAAAAAAAAAAAAAA

Probe-162:
AAATATCTTTAGGAAAAGCGTAAGAATACGTGGCACAGACAACCAACAGAG ATAGAAAAAA
AAAAAAAAAAAAAAAAAAAAAAAAAAAAAAAA

Probe-164:
ACCCTTCTGACCTGTTTATAATCAGTGAGGCCACCGAGTAAAACGGTACGCC AGAAAAAAA
AAAAAAAAAAAAAAAAAAAAAAAAAAAAAAAA

Probe-166:
TCCTGAGAAGTGTTCACTAAATCGGAACCCTAAAGGGAGCCCAGTTTTTTGG
GGTCAAAAAAAAAAAAAAAAAAAAAAAAAAAAAAAAAAAAA

Tri1 tile probe sequences:

Probe-A37:
AGAGAATAACATAAAAACAGGGAAGCGCATTAAAAAAAAAAAAAAAAAAA

AAAAAAAAAAAAAAAAAAAA

Probe-A33:
CCTTTTTTCATTTAACAATTTCATAGGATTAGAAAAAAAAAAAAAAAAAAAA
AAAAAAAAAAAAAAAAAAAA

Probe-A10:
TGTACTGGAAATCCTCATTAAAGCAGAGCCACAAAAAAAAAAAAAAAAAAAA
AAAAAAAAAAAAAAAAAAAA

Probe-A39:
TTATCAAACCGGCTTAGGTTGGGTAAGCCTGTAAAAAAAAAAAAAAAAAAAA
AAAAAAAAAAAAAAAAAAAA

Probe-A35:
AGTATAAAATATGCGTTATACAAAGCCATCTTAAAAAAAAAAAAAAAAAAAA
AAAAAAAAAAAAAAAAAAAA

Tri3 tile probe sequences:

Probe-A37:
AGAGAATAACATAAAAACAGGGAAGCGCATTAAAAAAAAAAAAAAAAAAAA
AAAAAAAAAAAAAAAAAAAA

Probe-A33:
CCTTTTTTCATTTAACAATTTCATAGGATTAGAAAAAAAAAAAAAAAAAAAA
AAAAAAAAAAAAAAAAAAAA

Probe-A10:
TGTACTGGAAATCCTCATTAAAGCAGAGCCACAAAAAAAAAAAAAAAAAAAA
AAAAAAAAAAAAAAAAAAAA

Probe-A39:
TTATCAAACCGGCTTAGGTTGGGTAAGCCTGTAAAAAAAAAAAAAAAAAAAA
AAAAAAAAAAAAAAAAAAAA

Probe-A35:
AGTATAAAATATGCGTTATACAAAGCCATCTTAAAAAAAAAAAAAAAAAAAA
AAAAAAAAAAAAAAAAAAAA

Probe-B37:
ACAGGTAGAAAGATTCATCAGTTGAGATTTAGAAAAAAAAAAAAAAAAAAAA
AAAAAAAAAAAAAAAAAAAA

Probe-B33:
AGGGATAGCTCAGAGCCACCACCCCATGTCAAAAAAAAAAAAAAAAAAAAA
AAAAAAAAAAAAAAAAAAAA

Probe-B10:
CAATATGACCCTCATATATTTTAAAGCATTAAAAAAAAAAAAAAAAAAAAAA
AAAAAAAAAAAAAAAAAAAA

Probe-B39:
ATTTTCTGTCAGCGGAGTGAGAATACCGATATAAAAAAAAAAAAAAAAAAAA
AAAAAAAAAAAAAAAAAAAA

Probe-B35:
GCCGCTTTGCTGAGGCTTGCAGGGGAAAAGGTAAAAAAAAAAAAAAAAAAAA
AAAAAAAAAAAAAAAAAAAA

Probe-C37:
CGAGAAAGGAAGGGAAGCGTACTATGGTTGCTAAAAAAAAAAAAAAAAAAAA
AAAAAAAAAAAAAAAAAAAA

Probe-C33:
CGCGTCTGATAGGAACGCCATCAACTTTTACAAAAAAAAAAAAAAAAAAAAA
AAAAAAAAAAAAAAAAAAAA

Probe-C10:
TAATCCTGATTATCATTTTGCGGAGAGGAAGGAAAAAAAAAAAAAAAAAAAA
AAAAAAAAAAAAAAAAAAAA

Probe-C39:
CAGTTTGACGCACTCCAGCCAGCTAAACGACGAAAAAAAAAAAAAAAAAAAA
AAAAAAAAAAAAAAAAAAAA

Probe-C35:
CTCTAGAGCAAGCTTGCATGCCTGGTCAGTTGAAAAAAAAAAAAAAAAAAAA
AAAAAAAAAAAAAAAAAAAA

E and M tile array linker sequences:

L1: CACCAACTACGTAA TGCCACT TCGGCTGTCTTTCC
L2: GAACCGGCATCAAG AGTAATC AGCCTGTTTAGTAT
L3: ACTAATGGATTTAG GAATACC TTTCCCTTAGAATC
L4: AGTCAGAGGTCTTT ACCCTGA AATAAAGAAATTGC
L5: ATTCTGCCCATATA ACAGTTG GCACTAACAACTAA
L6: GTAGATTTTCAGGTTATCAAAATTATTT GCACGTAAAACAGA CTATTAT
L7: CTTGAAAACATAGCCTTCTGTAAATCGT CGCTATTAATTAAT ACATTCA
L8: CATATGCGTTATACAAACACCGGAATCA TAATTACTAGAAAA TTGACAA
L9: TTATCATTCCAAGATTACGAGCATGTAG AAACCAATCAATAA ACGAAGG
L10: TAGATTAGAGCCGTAGGAAGGTTATCTAAAATATCTTTAGGA ATTCCCA

References:

1.) Laemmli, U.K. *Nature* **1970**, *227*, 680-685.
2.) Rothemund, P.W.K. *Nature* **2006**, *440*, 297-302.
3.) Carrico, Z.M.; Romanini, D.W.; Mehl, R.A.; Francis, M.B. *Chem. Commun.* **2008**, 1205-1207.
4.) Stephanopoulos, N.; Carrico, Z.M.; Francis, M.B. *Angew. Chem. Int. Ed.* **2009**, *48*, 9498-9502.
5.) Tong, G.J.; Hsiao, S.C.; Carrico, Z.M.; Francis, M.B. *J. Am. Chem. Soc.* **2009**, *131*, 11174-11178.

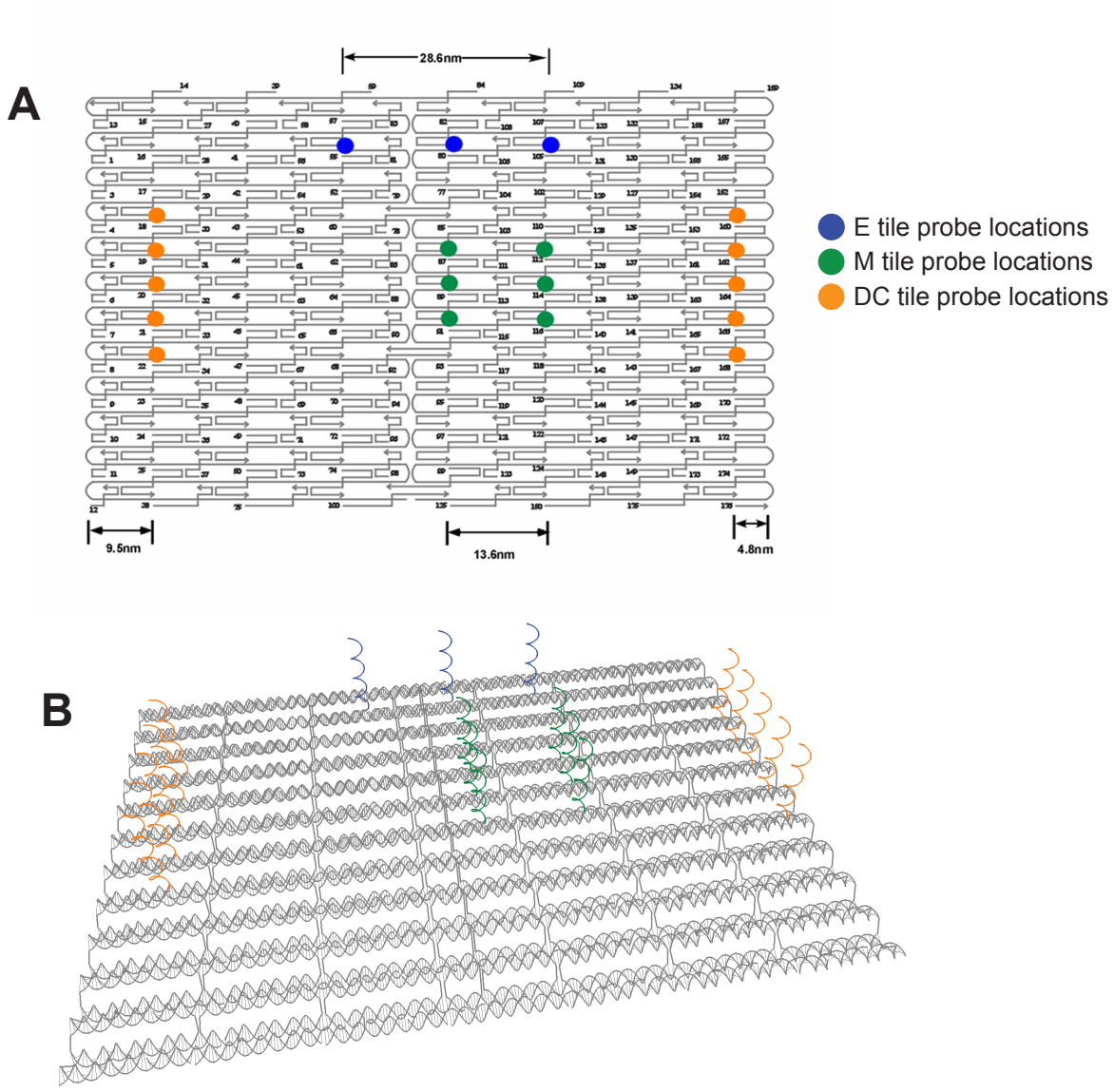

Figure S1. Schematic representation of the rectangular tiles used in this study. (A) Digram showing the location of the probes in the three designs. Numbers refer to the staples holding together the M13 backbone. (B) Image of rectangular tile showing all the helices as well as the protruding probes for the three designs. The 3' end of each probe is protruding from the tile.

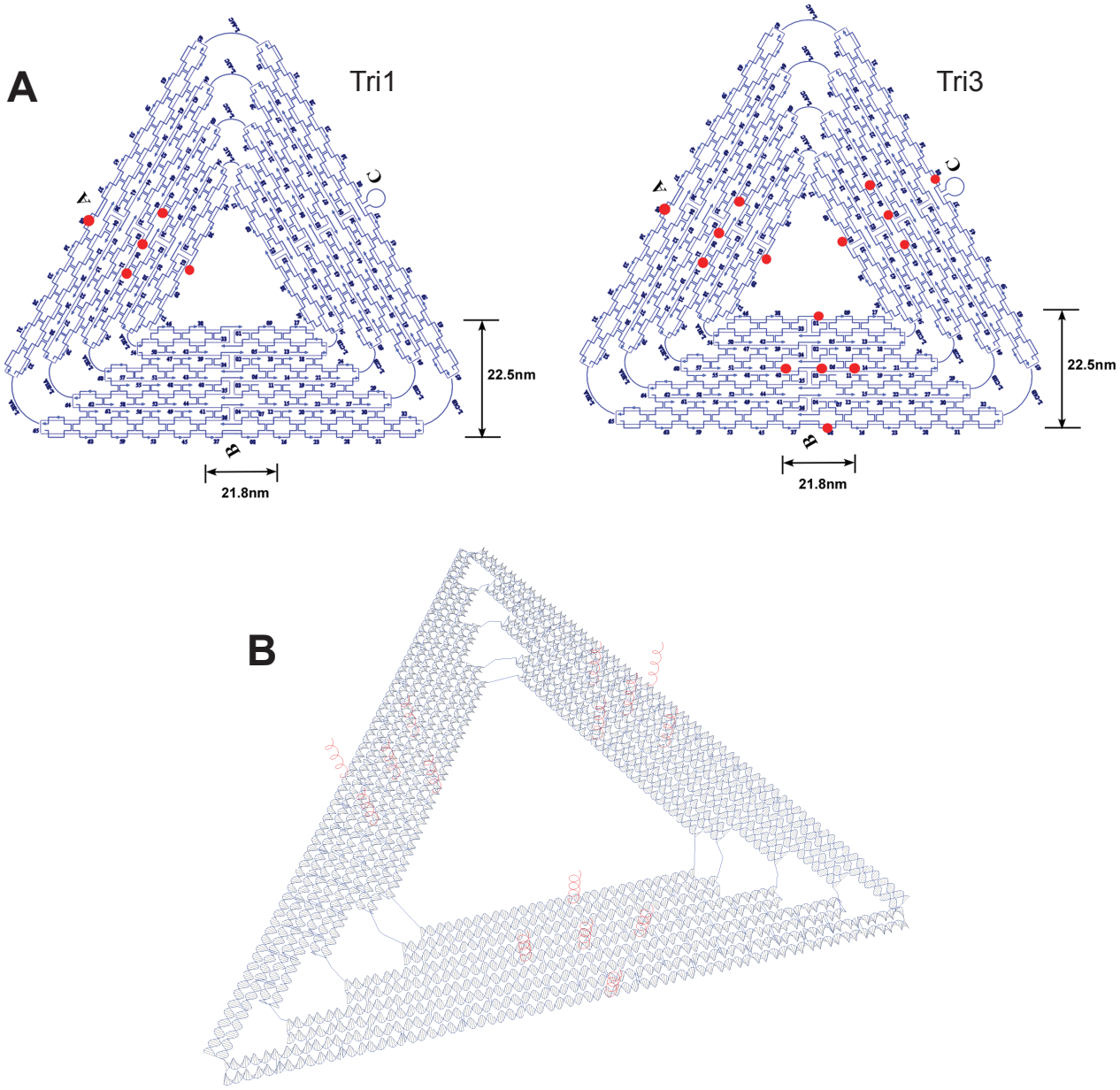

Figure S2. Schematic representation of the triangular tiles used in this study. (A) Diagram showing the location of the probes (red dots) in the two triangle designs. Numbers refer to the staples holding together the M13 backbone. (B) Image of the Tri3 tile showing all the helices as well as the protruding probes. The design of the Tri1 tile was identical, but with only one set of probes. The 3' end of each probe is protruding

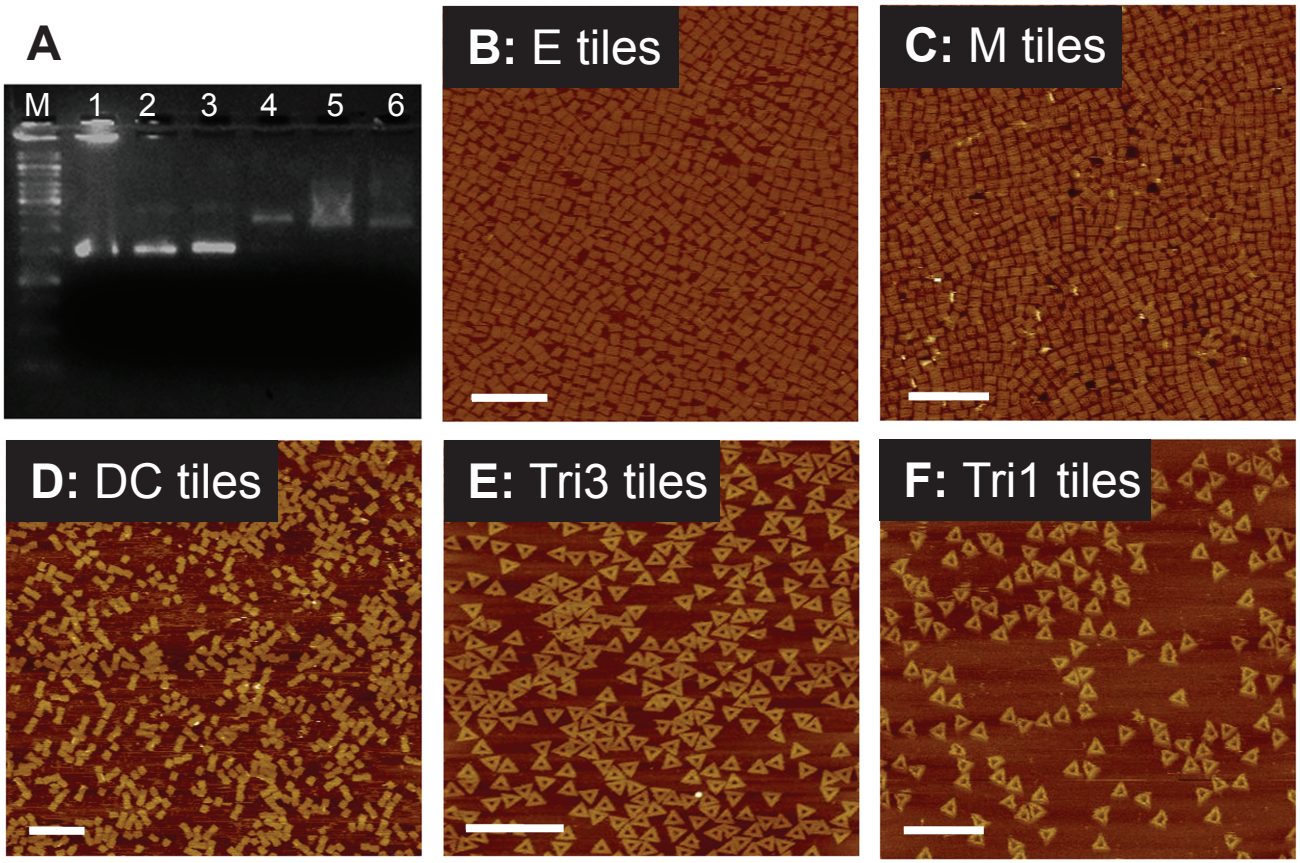

Figure S3. Characterization of the origami tiles. (A) Agarose gel of the tiles used in this paper. Lanes: M: 1 kb ladder, 1: M13 genome, 2: E tiles, 3: M tiles, 4: DC tiles (dimer due to edge stacking), 5: Tri1 tiles, 6: Tri3 tiles. (B-F): AFM images of single tiles after purification. Scale bars: 500 nm.

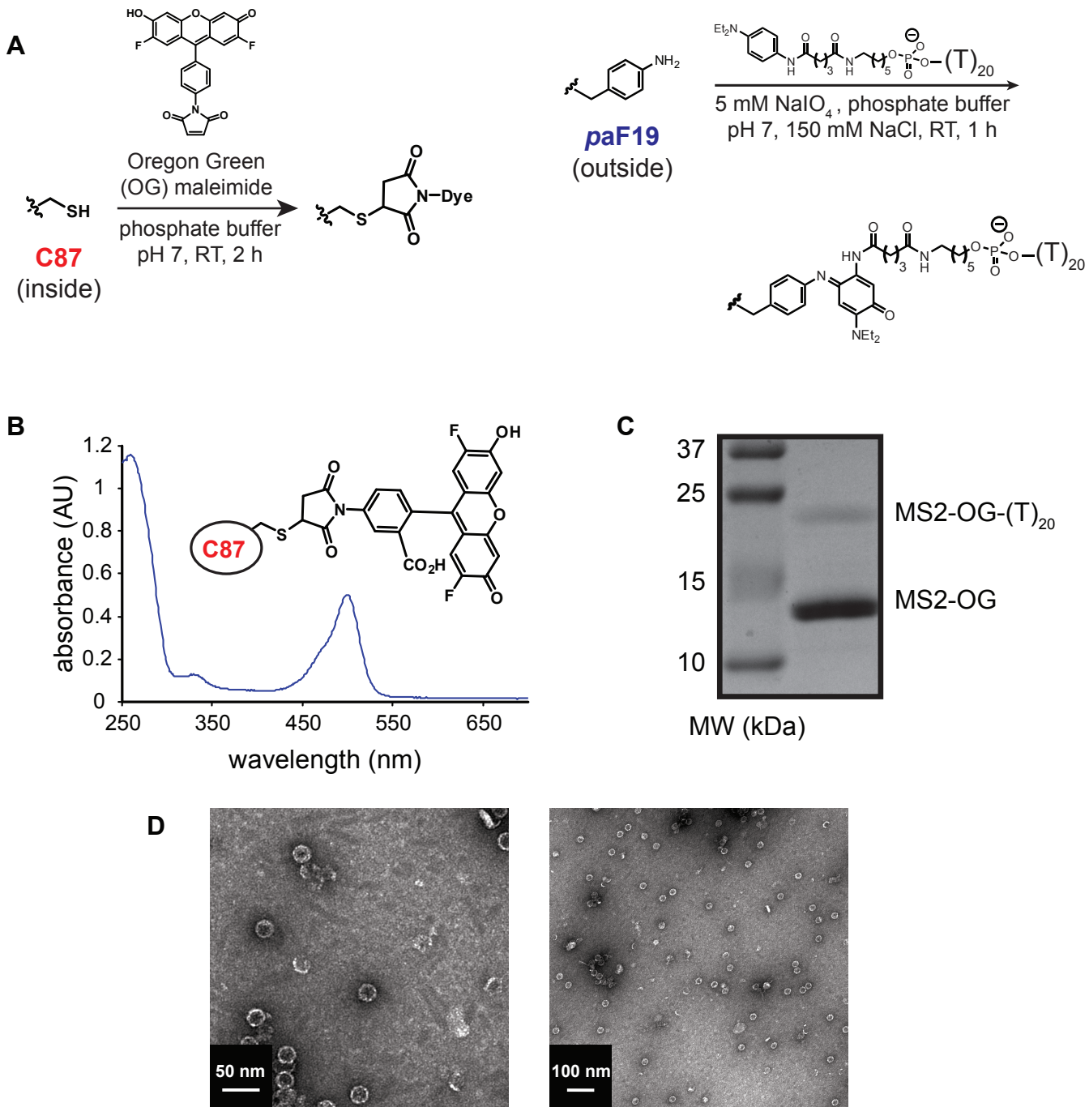

Figure S4. Synthesis and characterization of the MS2 capsids with Oregon Green (OG) inside and ssDNA outside. The 5' end of the ssDNA strand is attached to the capsid. (A) Synthetic scheme to modify the interior of the capsid with Oregon Green maleimide at C87 and the exterior of the capsid with $(T)_{20}$ DNA at the unnatural amino acid *p*aF19 using an oxidative coupling reaction. (B) The UV-Vis spectrum of the MS2-OG conjugate shows the chromophore absorbance at 500 nm. The conversion was estimated to be nearly quantitative by the comparison of the dye extinction coefficient ($\varepsilon_{500\ nm}$ = 80,000 $M^{-1}cm^{-1}$) and the protein's extinction coefficent ($\varepsilon_{260\ nm}$ = 176,000 $M^{-1}cm^{-1}$) . (C) SDS-PAGE analysis of the MS2-OG-$(T)_{20}$ conjugate shows a new band at higher molecular weight corresponding to the protein-DNA conjugate. The conversion was estimated to at ~11% by densitometry (corresponding to ~20 copies/capsid). (D) Transmission electron microscopy images of the MS2-OG-$(T)_{20}$ conjugate indicated that the capsids were intact, assembled, and 27 nm in diameter as expected

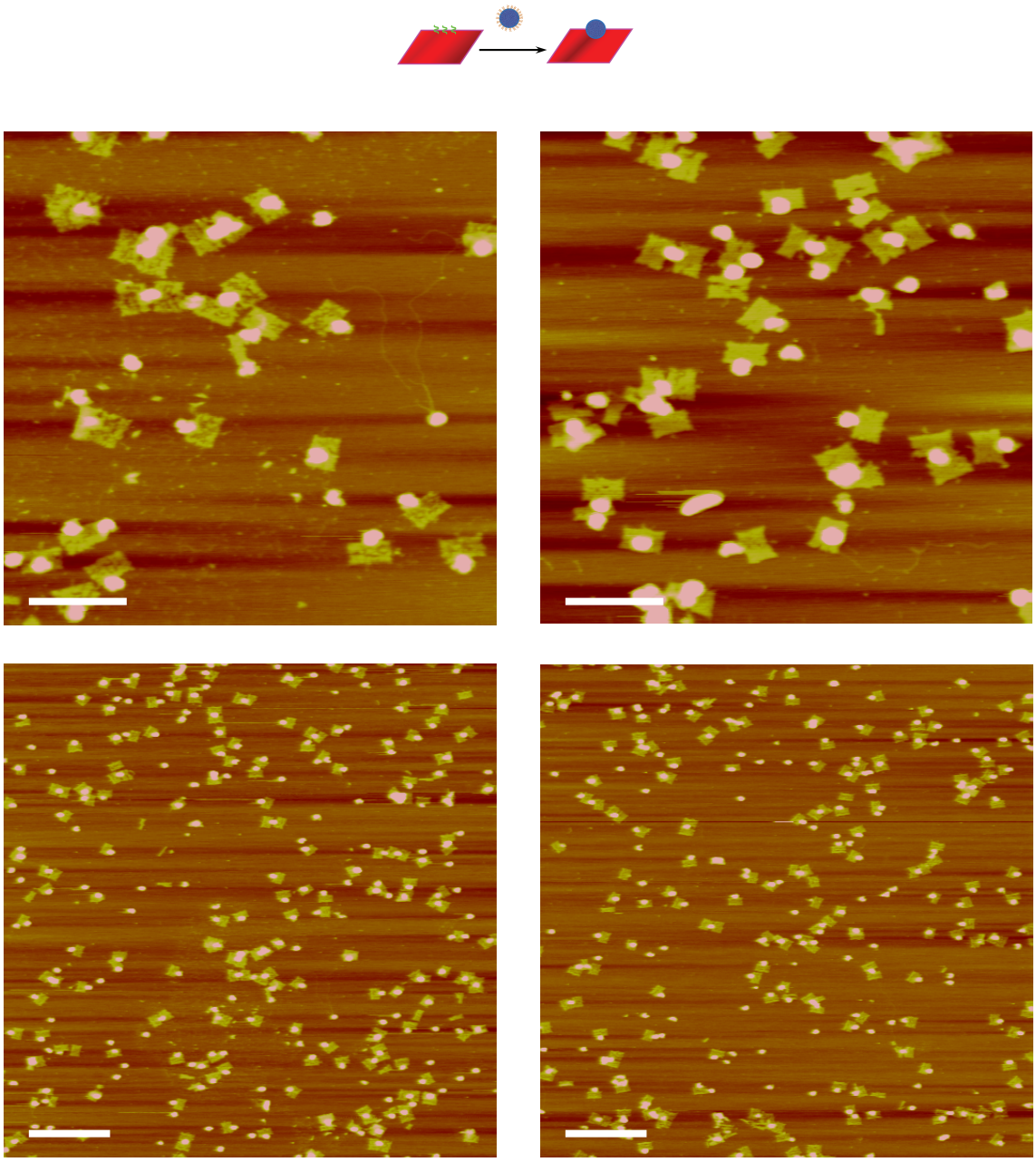

Figure S5. Additional AFM images of E tiles + MS2. Zoom-in scale bars: 200 nm. Zoom-out scale bars: 500 nm.

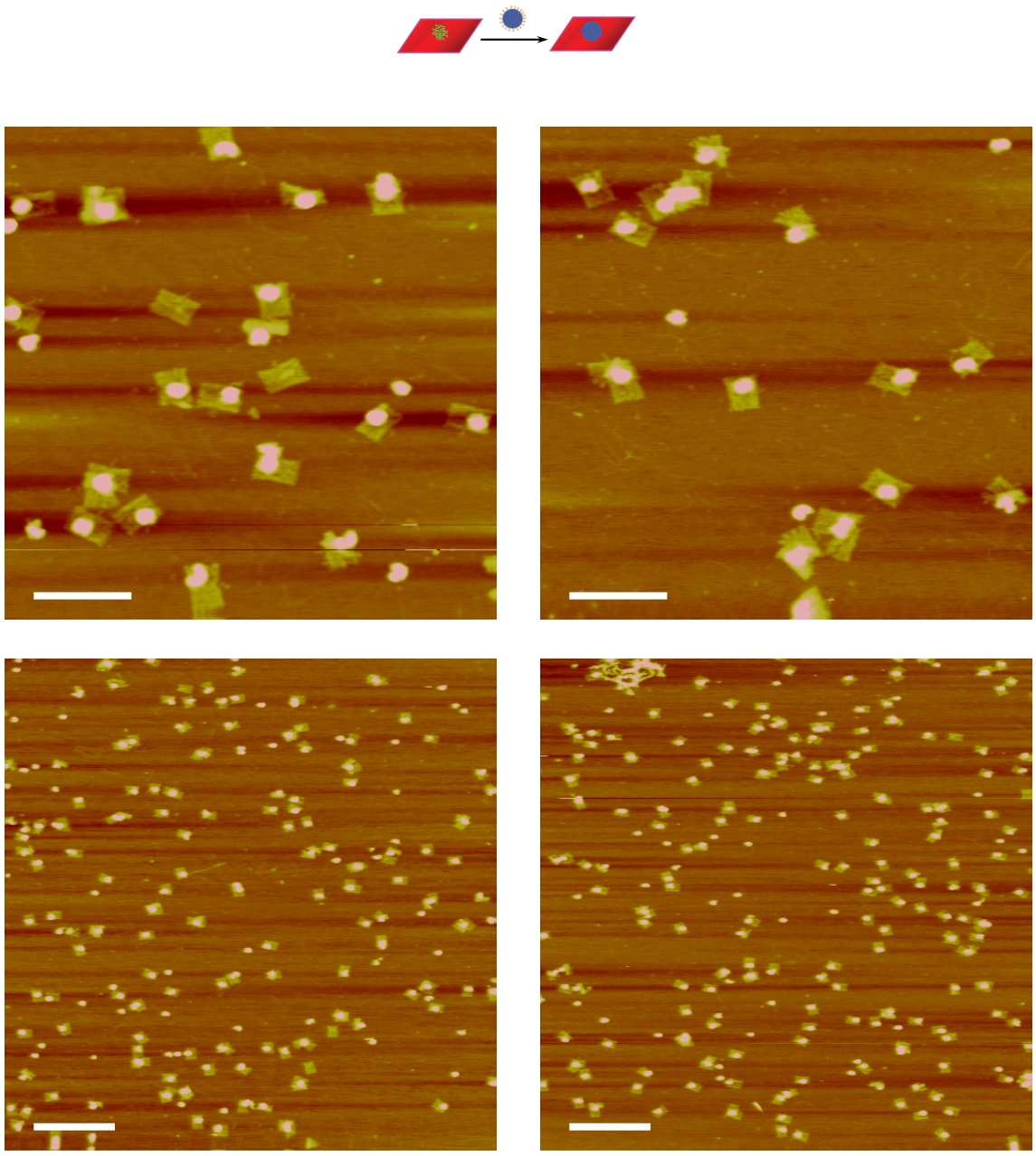

Figure S6. Additional AFM images of M tiles + MS2. Zoom-in scale bars: 200 nm. Zoom-out scale bars: 500 nm.

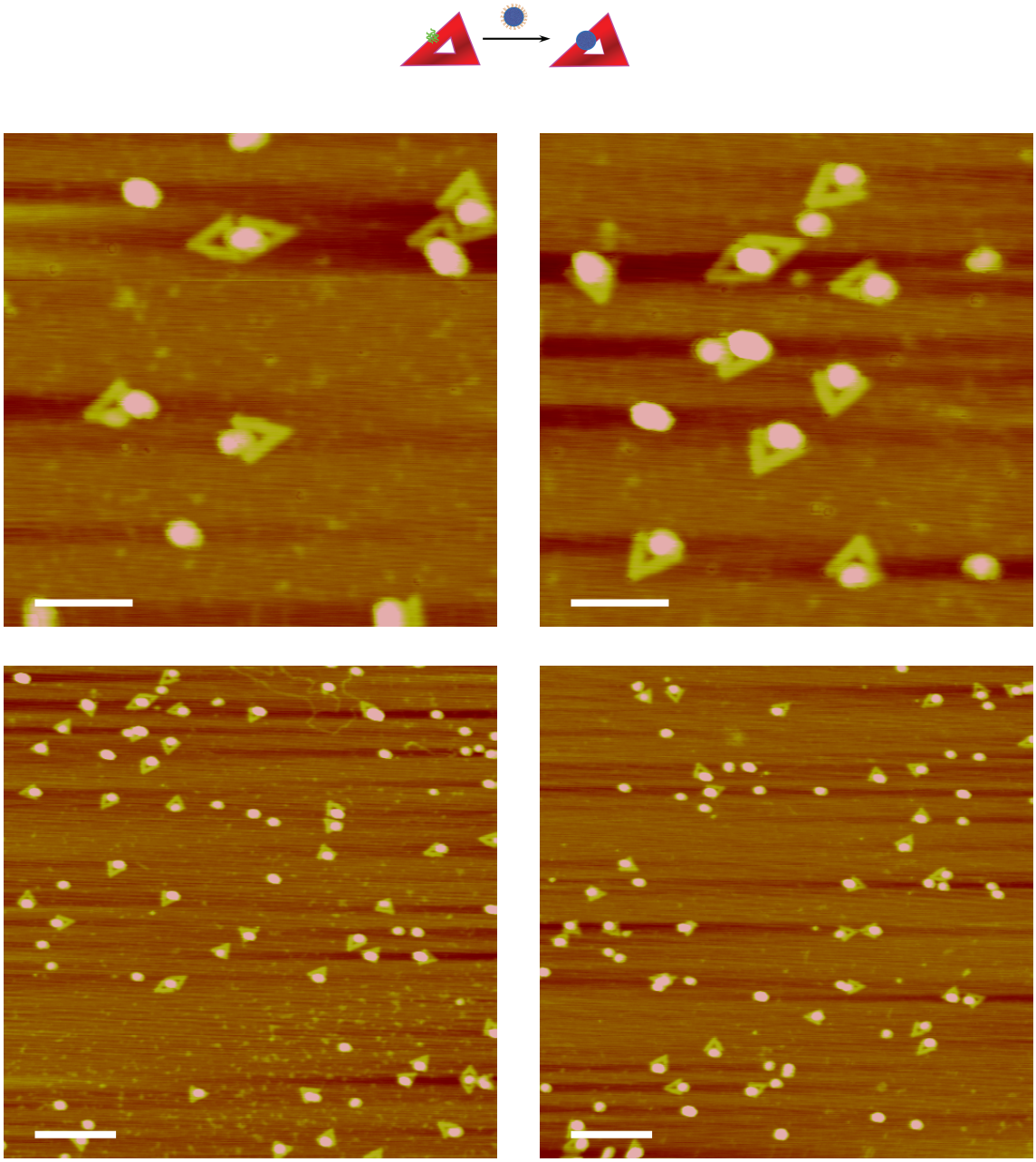

Figure S7. Additional AFM images of Tri1 tiles + MS2. Zoom-in scale bars: 200 nm. Zoom-out scale bars: 500 nm.

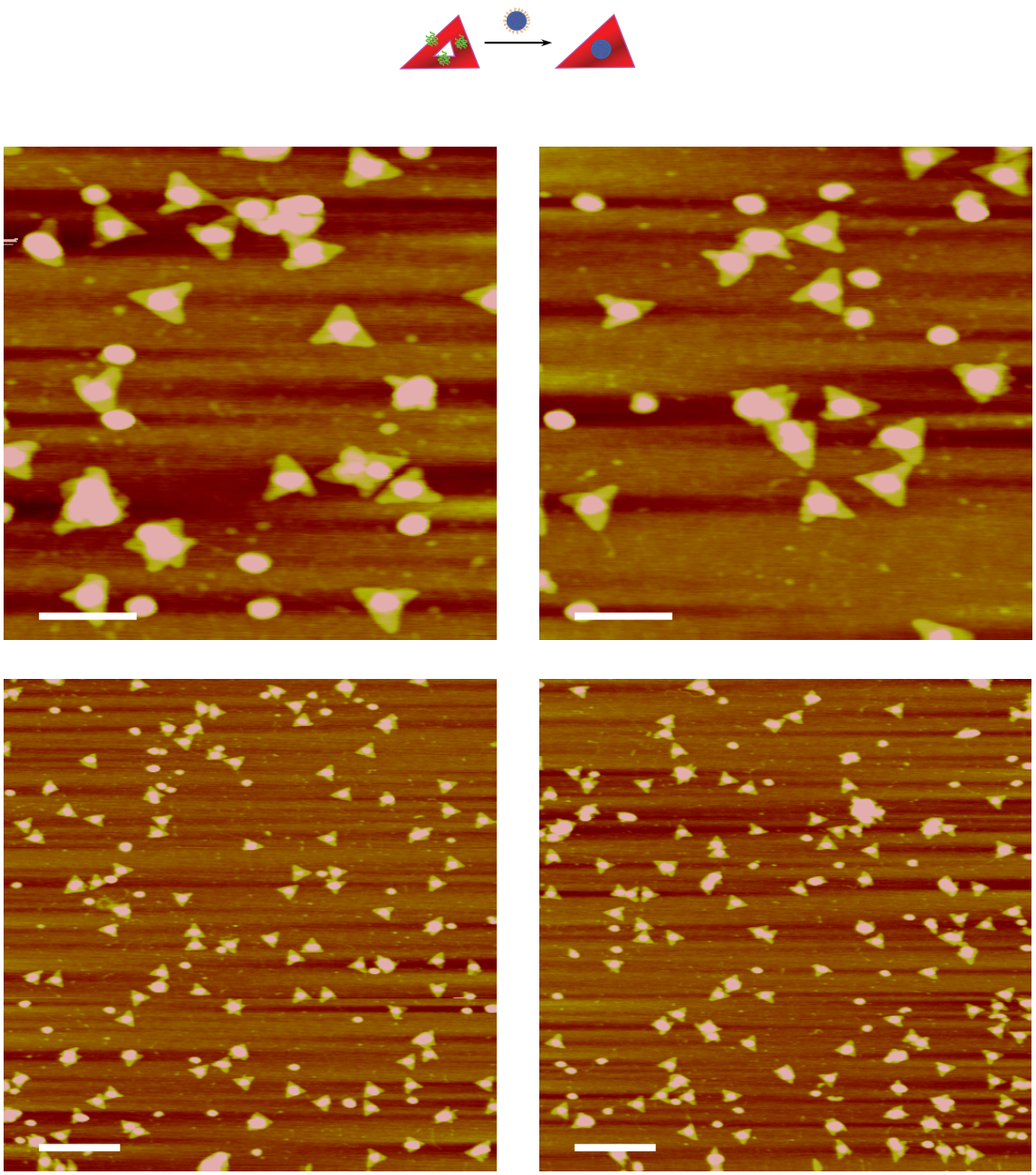

Figure S8. Additional AFM images of Tri3 tiles + MS2. Zoom-in scale bars: 200 nm. Zoom-out scale bars: 500 nm.

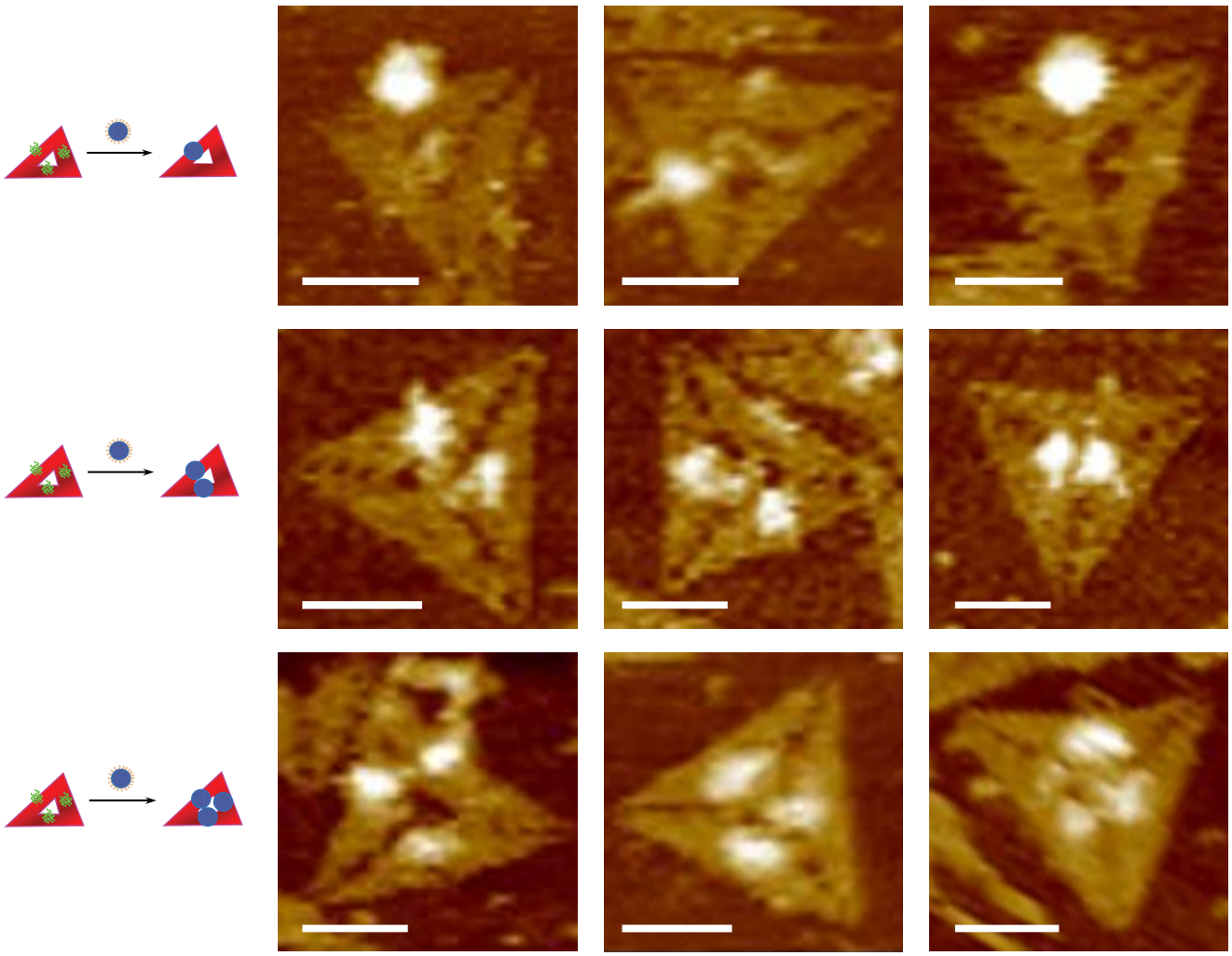

Figure S9. Additional AFM images of Tri3 tiles showing the occasional binding of one capsid to a single edge of the tile (but not sitting in the hole), two capsids binding to two edges of the tile, or three capsids binding to three edges of the tile. Scale bars: 50 nm.

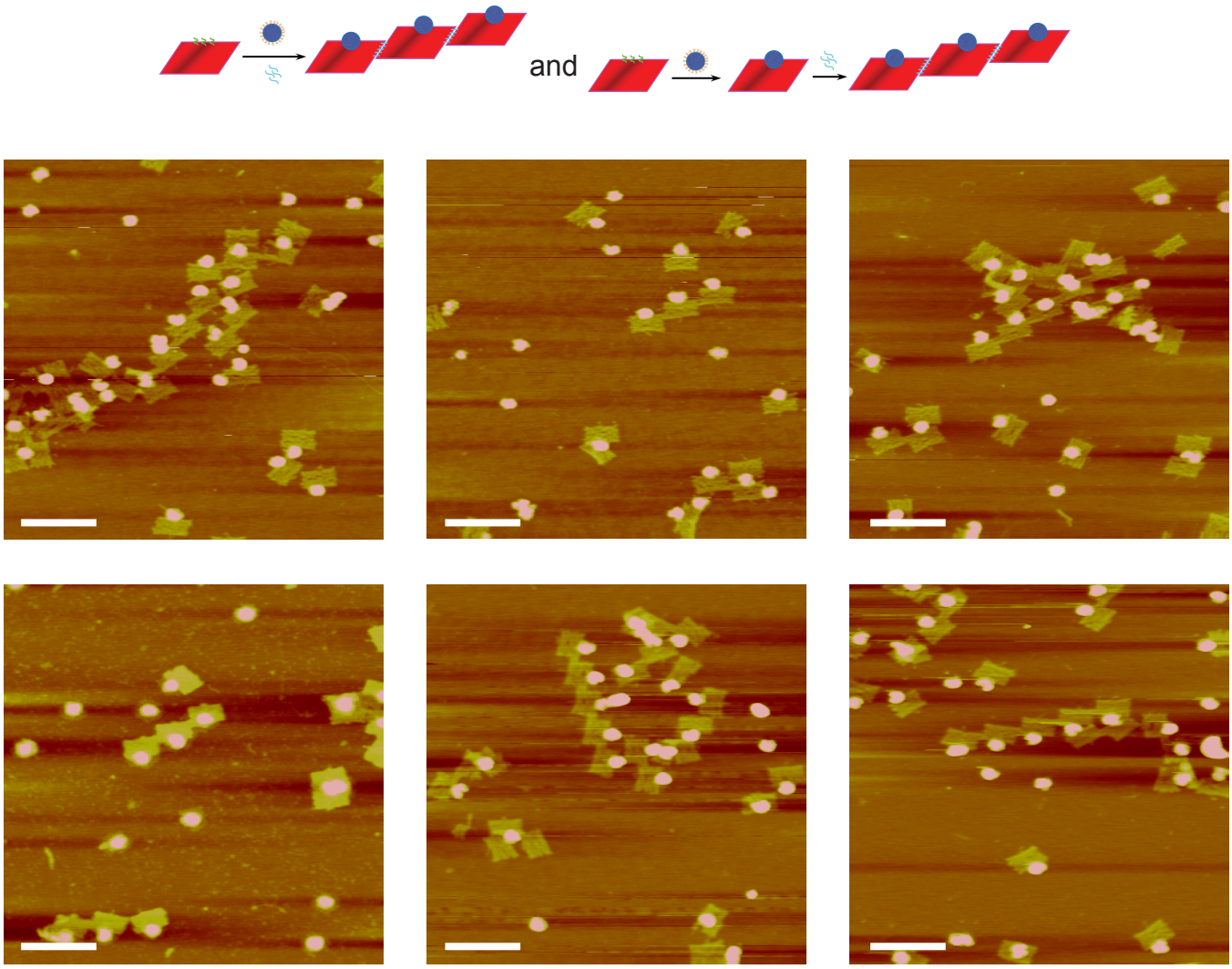

Figure S10. Additional AFM images of E tile arrays with MS2. Note the frequent occurence of array aggregation due to multiple tiles binding a single capsid. Scale bars: 200 nm.

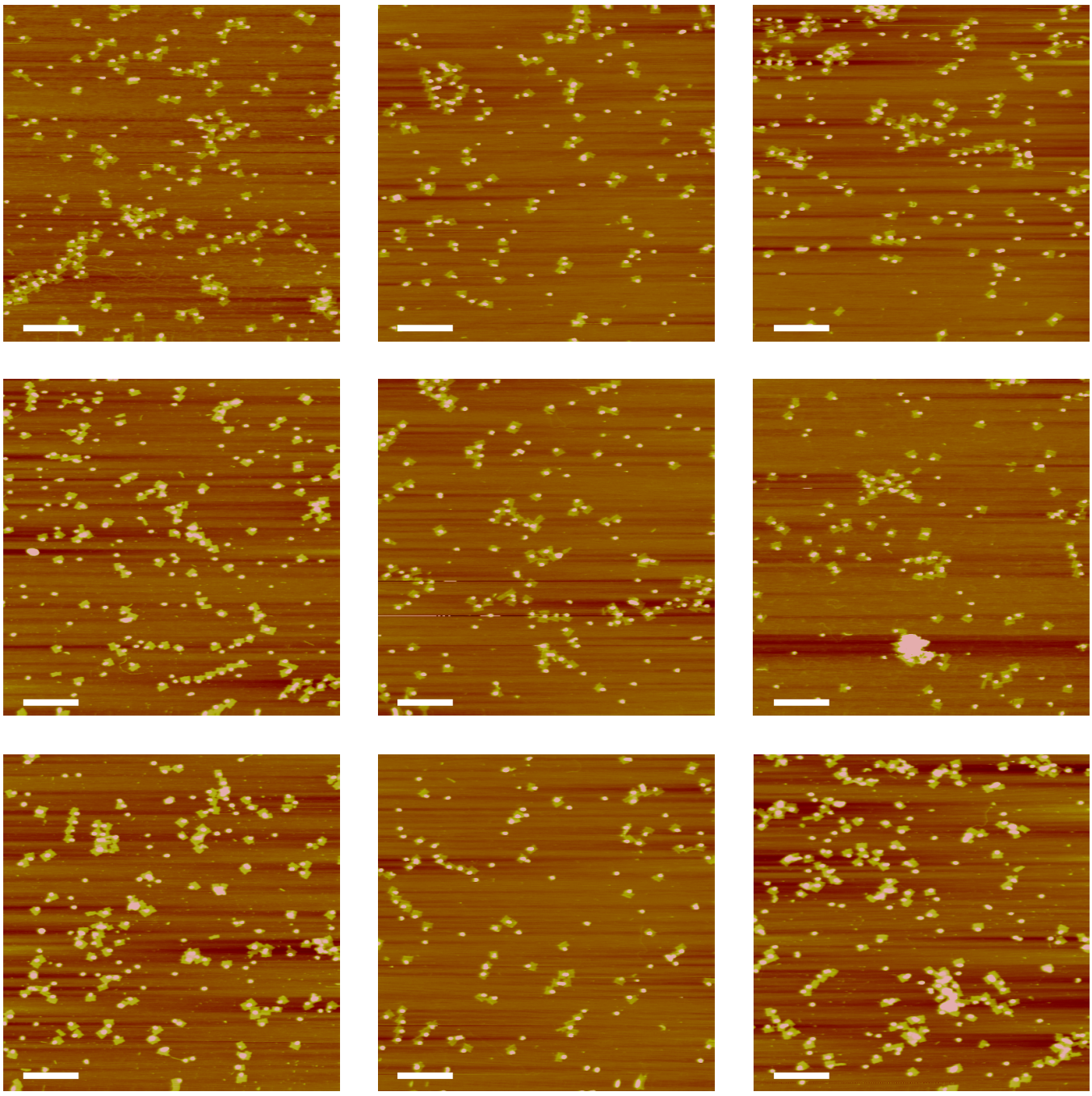

Figure S10 (cont). Additional AFM images of E tile arrays with MS2. Scale bars: 500 nm.

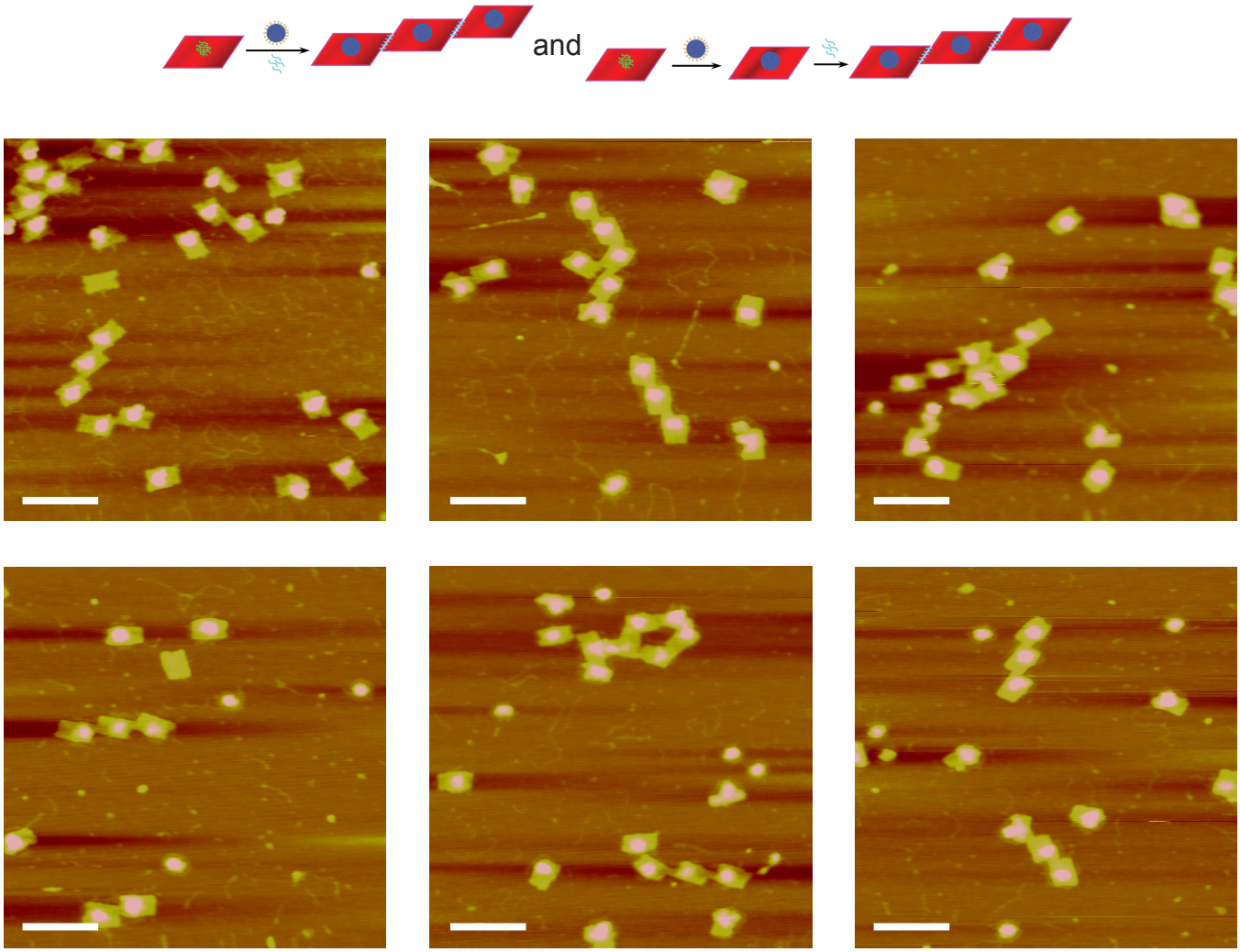

Figure S11. Additional AFM images of M tile arrays with MS2. Scale bars: 200 nm.

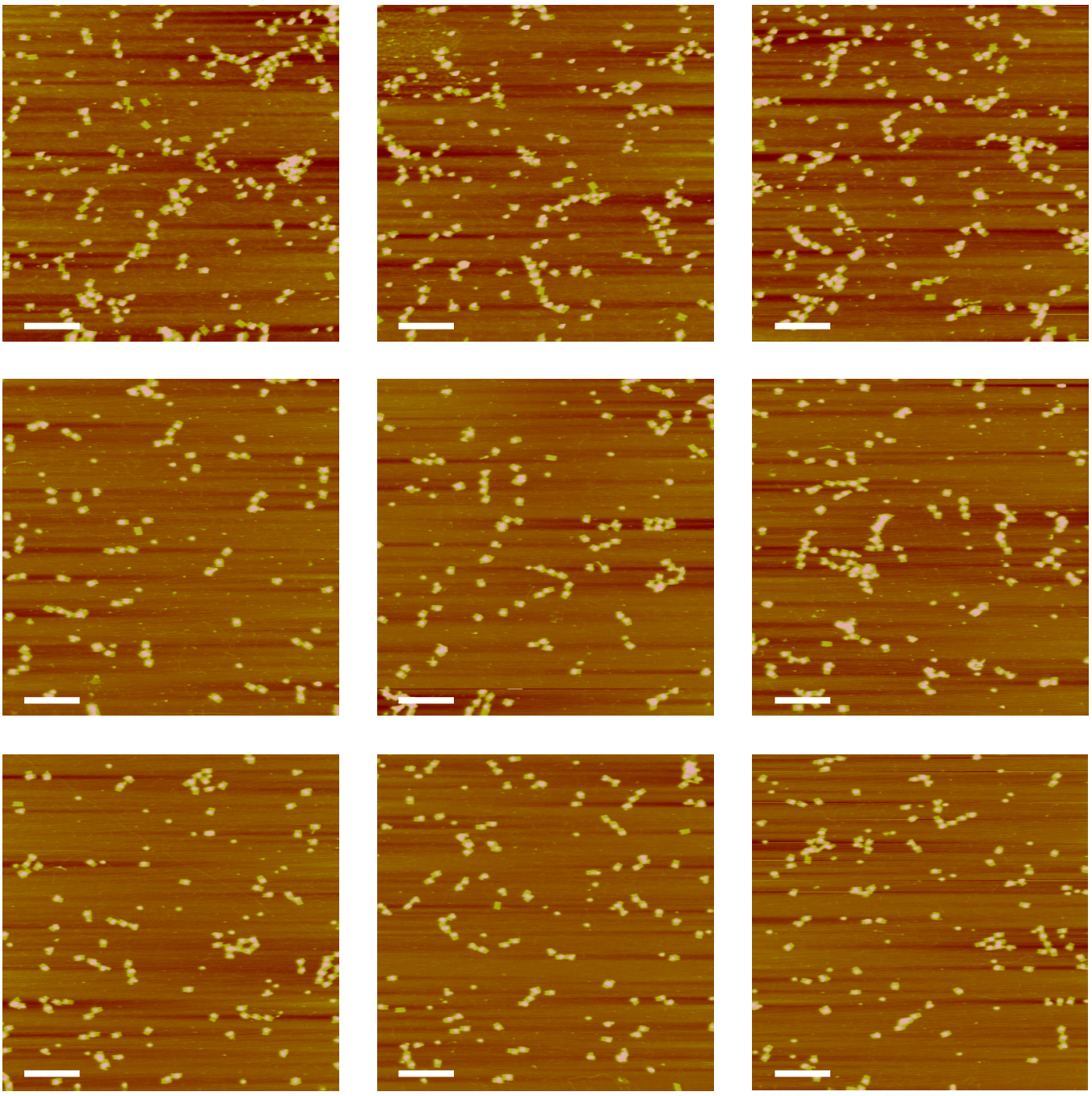

Figure S11 (cont). Additional AFM images of M tile arrays with MS2. Scale bars: 500 nm.

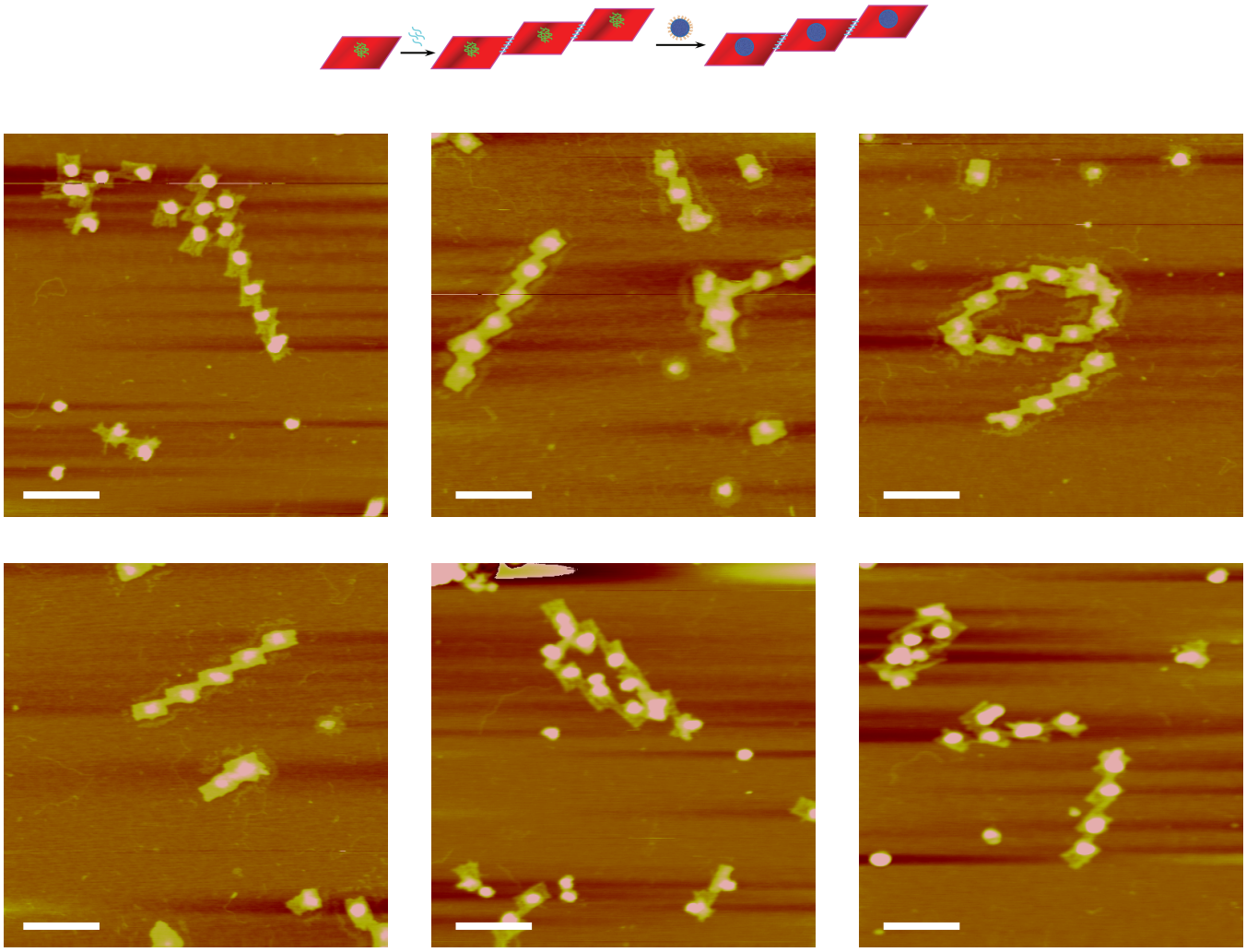

Figure S11 (cont). Additional AFM images of M tile arrays with MS2. Scale bars: 200 nm.

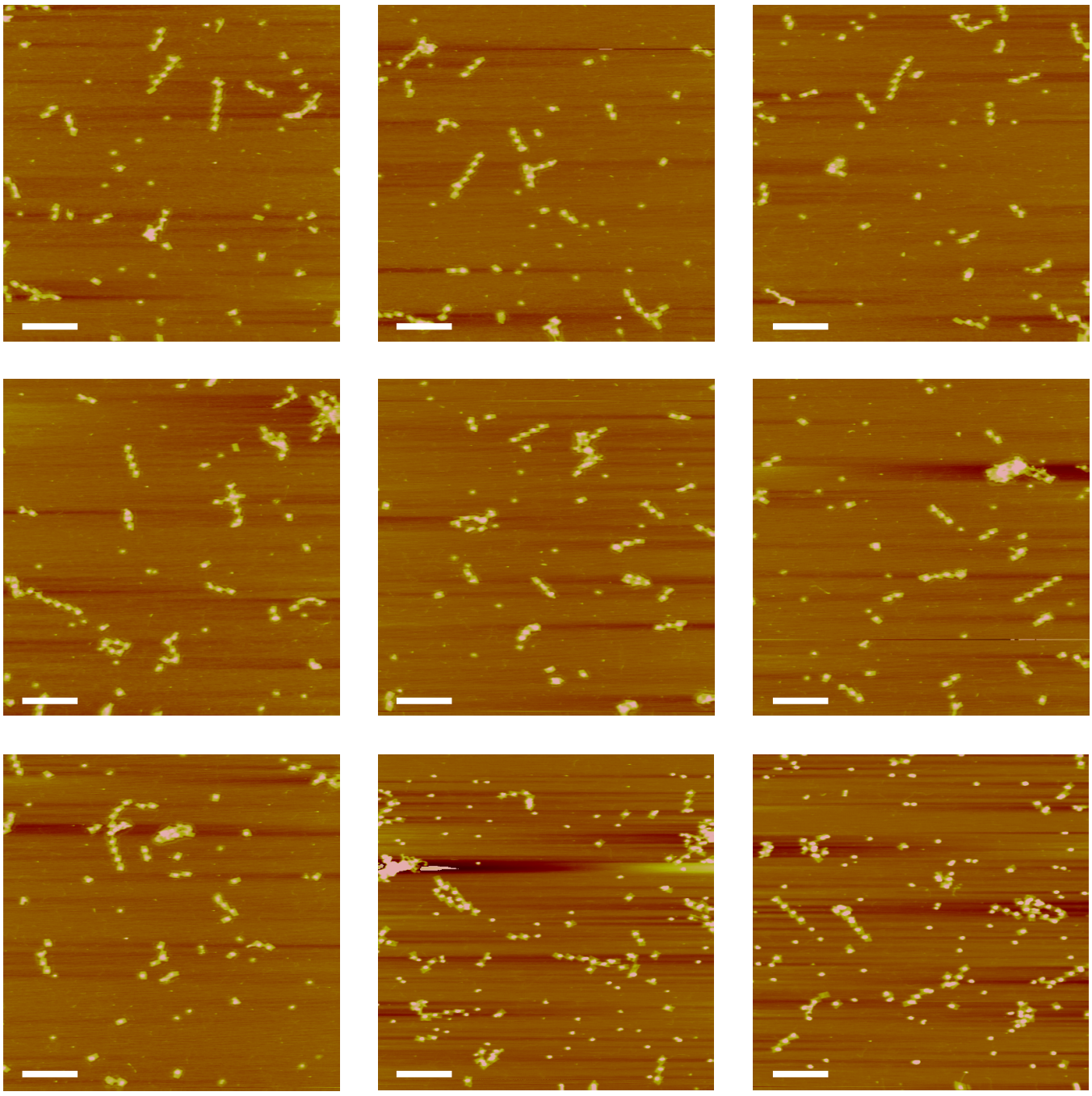

Figure S11 (cont). Additional AFM images of M tile arrays with MS2 . Scale bars: 500 nm.

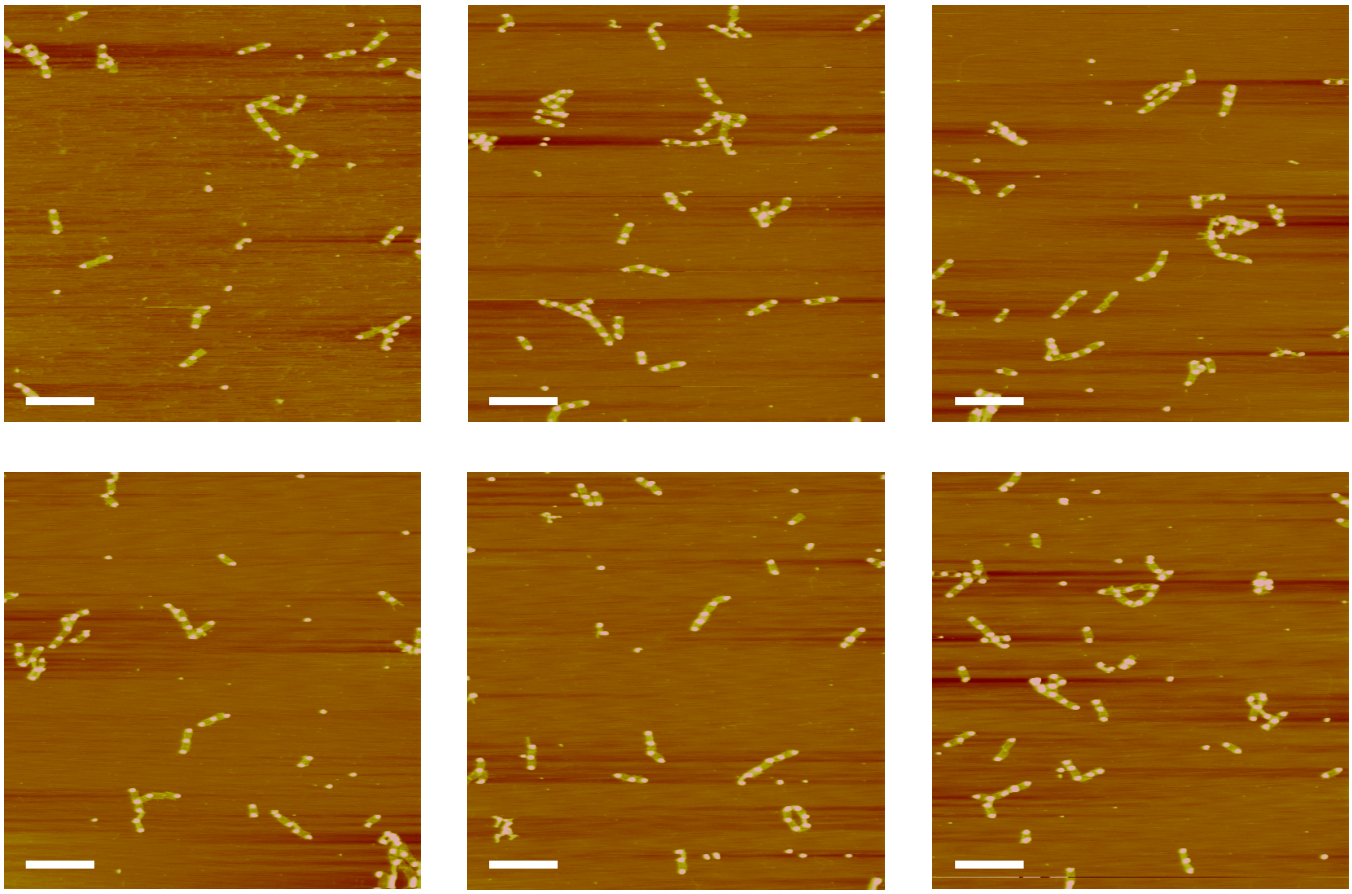

Figure S12. AFM images of additional DC tile arrays formed with MS2. Scale bars: 500 nm.

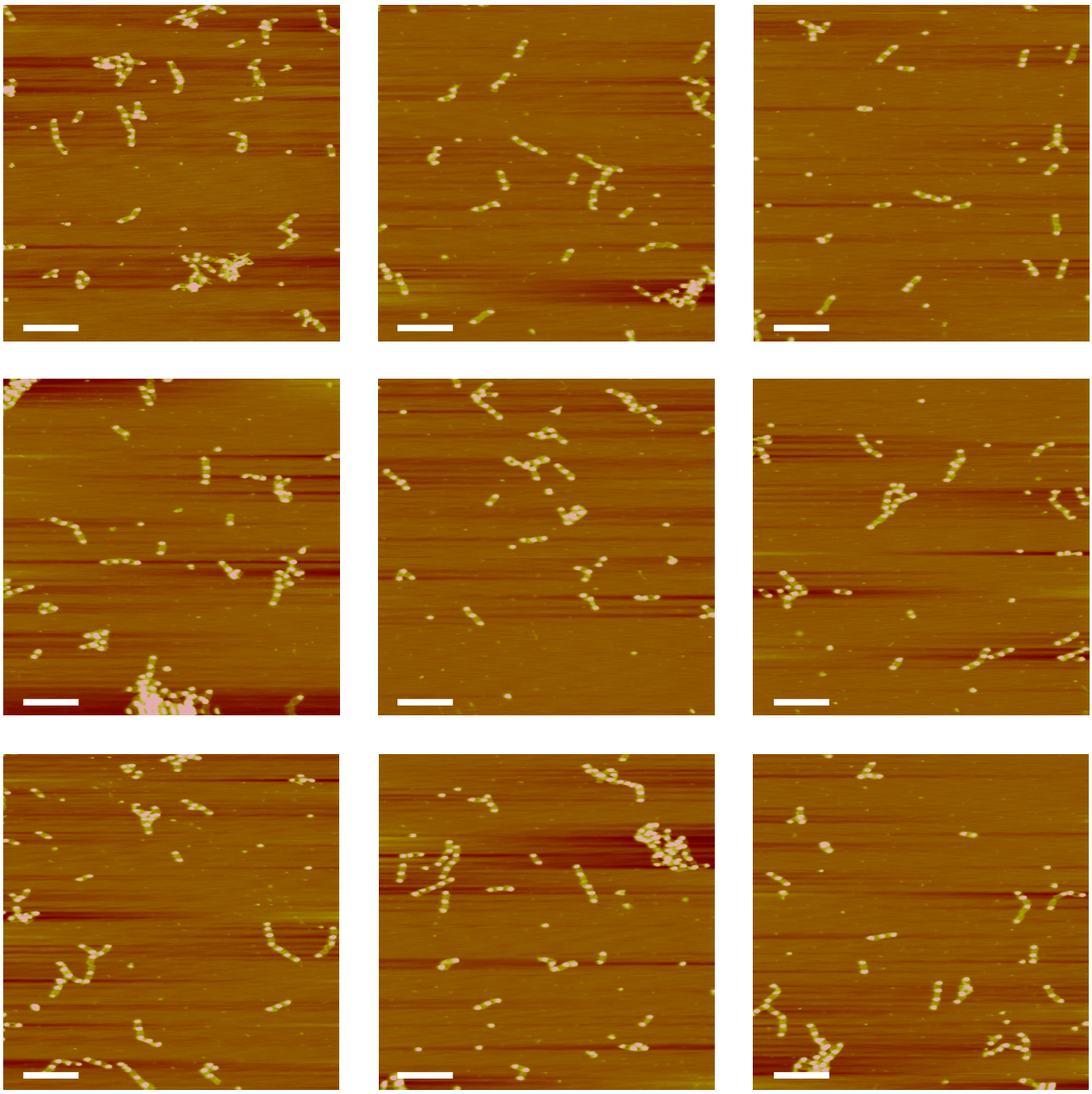

Figure S12 (cont). AFM images of additional DC tile arrays formed with MS2. Scale bars: 500 nm.

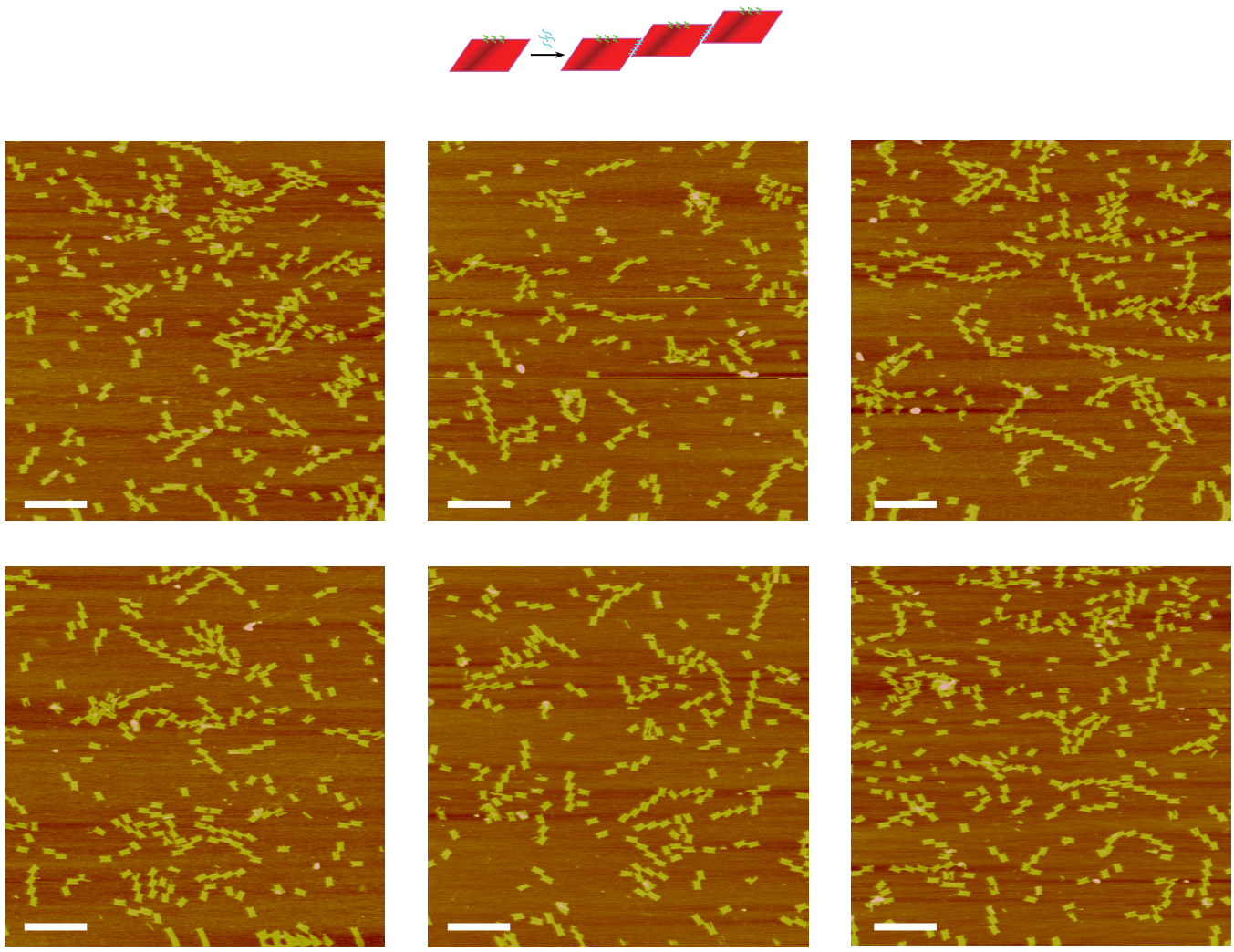

Figure S13. AFM images of E tile arrays formed without MS2. Scale bars: 500 nm.

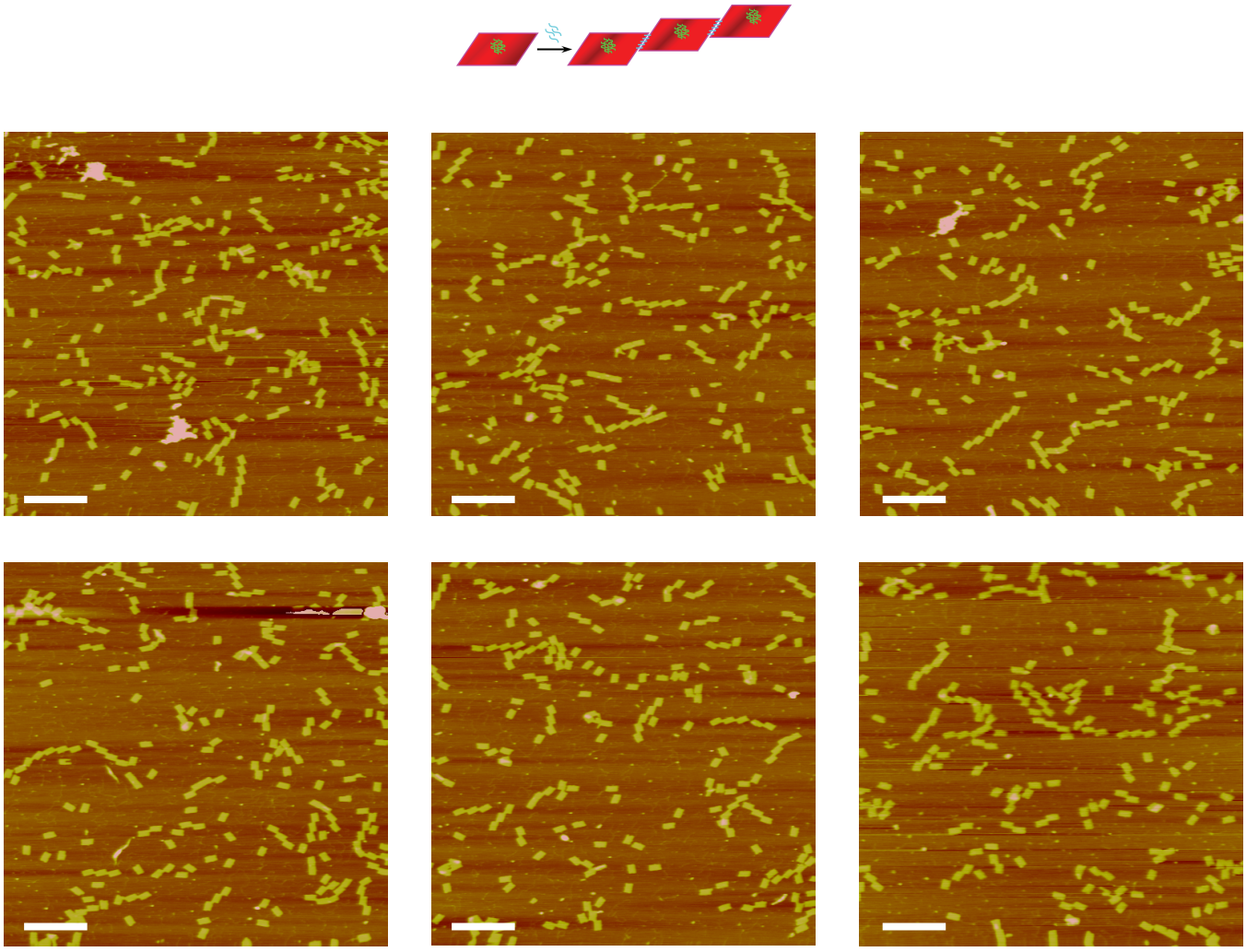

Figure S14. AFM images of M tile arrays formed without MS2. Scale bars: 500 nm.

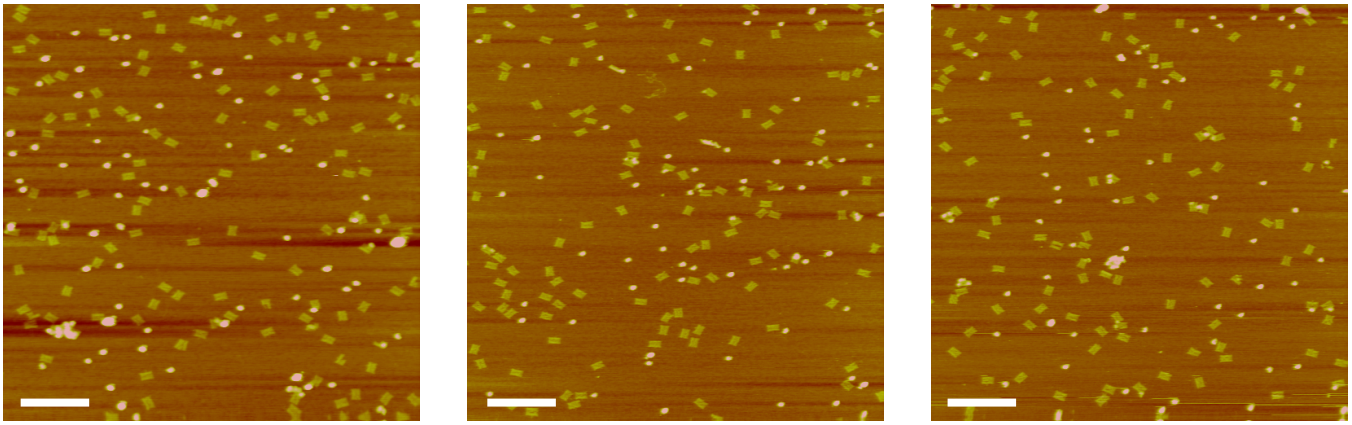

Figure S15. AFM images of control experiment: E tiles with MS2-dye (no DNA). No significant association of the capsids with the tiles is visible. Scale bars: 500 nm.

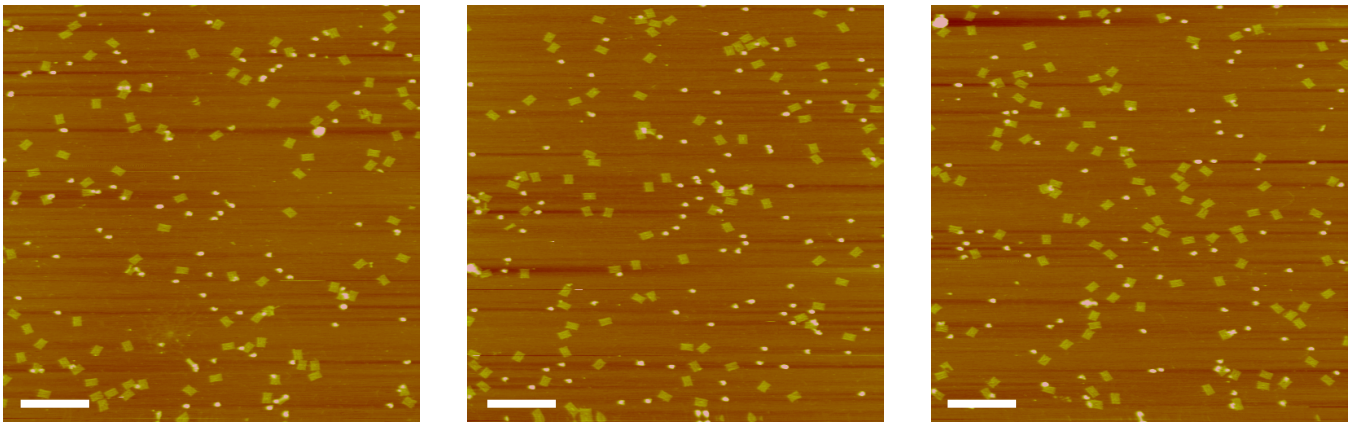

Figure S16. AFM images of control experiment: M tiles with MS2-dye (no DNA). No significant association of the capsids with the tiles is visible. Scale bars: 500 nm.

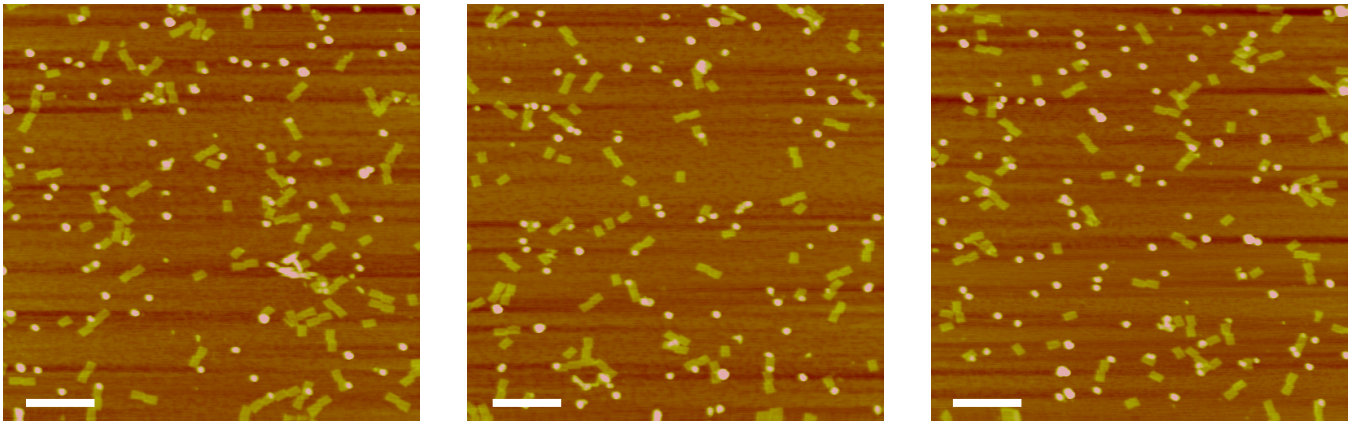

Figure S17. AFM images of control experiment: DC tiles with MS2-dye (no DNA) + edge staples. No significant association of the capsids with the tiles is visible. Note the prevalent association of the tile short edges to due noncovalent base stacking induced by the edge staples. Scale bars: 500 nm.

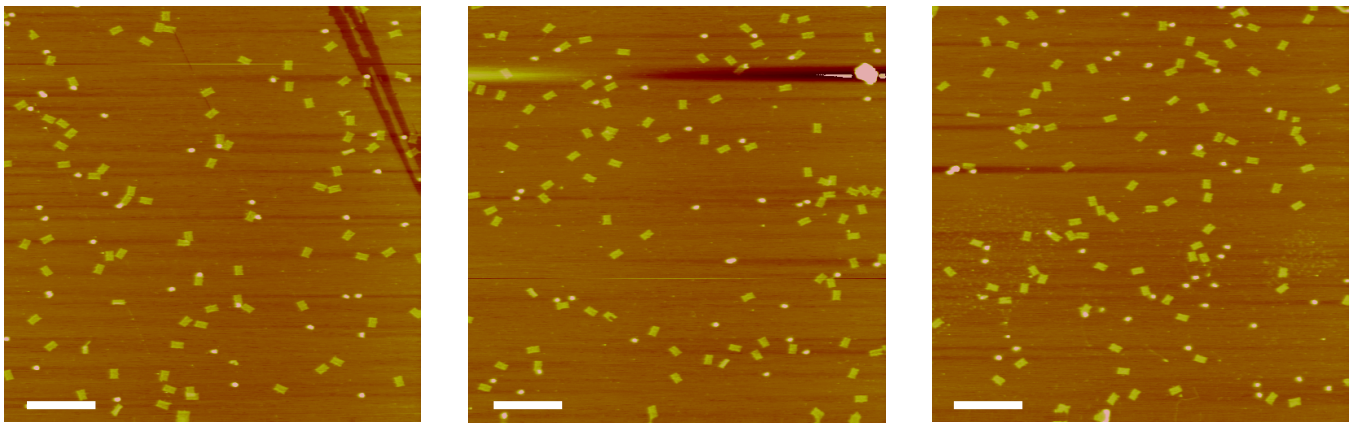

Figure S18. AFM images of control experiment: E tiles with capsids, but with mismatched probes. The capsids contained the 20-bp polyT sequence, but the tiles contained probes with a random 40-bp sequence. No association is seen between the capsids and the tiles, further indicating that specific DNA hybridization is necessary and the association is not a non-specific DNA-based effect. Scale bars: 500 nm.

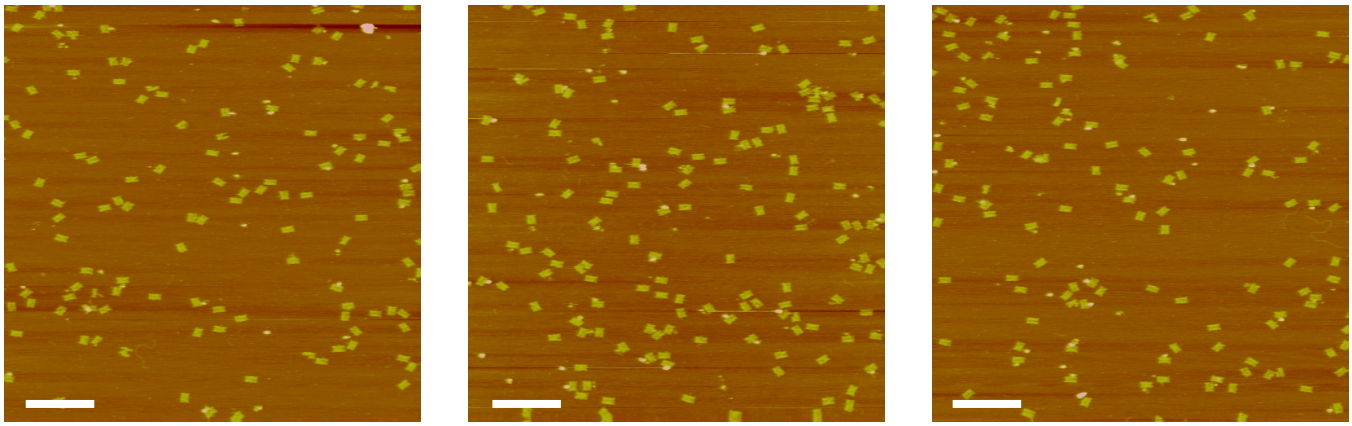

Figure S19. Control experiments: E tiles with capsids with matched probes, then addition of excess $(T)_{40}$ strand. Very few tiles still have capsids bound to them, indicating both the sequence selective nature of the capsid-tile association, as well as suggesting a release mechanism for capsids once bound to the tiles. Fewer capsids are seen on the surface than usual, likely due to passivation of the mica by the excess ssDNA, thus electrostatically occluding the surface to the capsids. Scale bars: 500 nm.

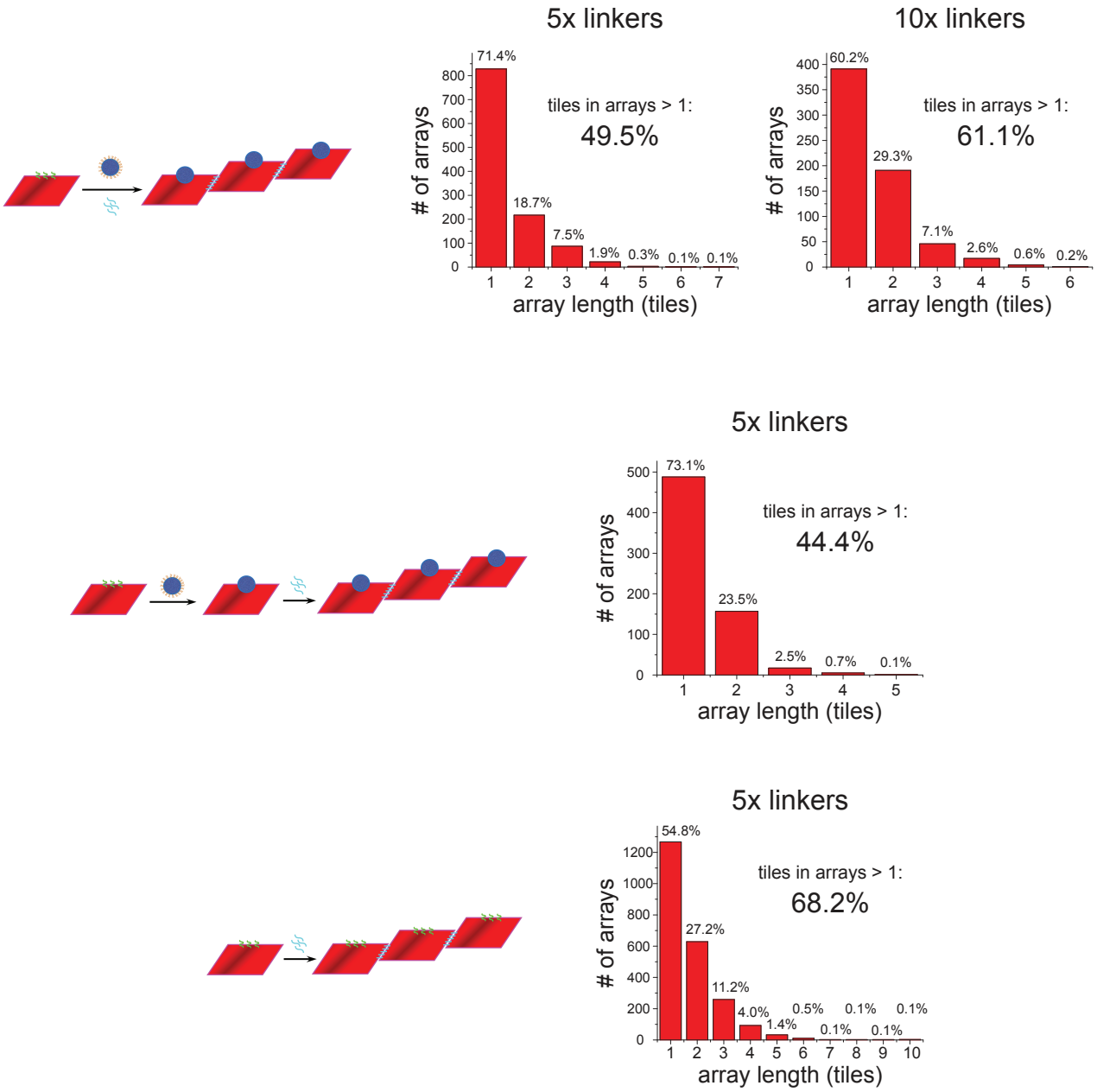

Figure S20. E tile array length distributions. An array length of 1 indicates a single tile not in an array. For the samples that include MS2, virtually complete association of the caspids with tiles was maintained.

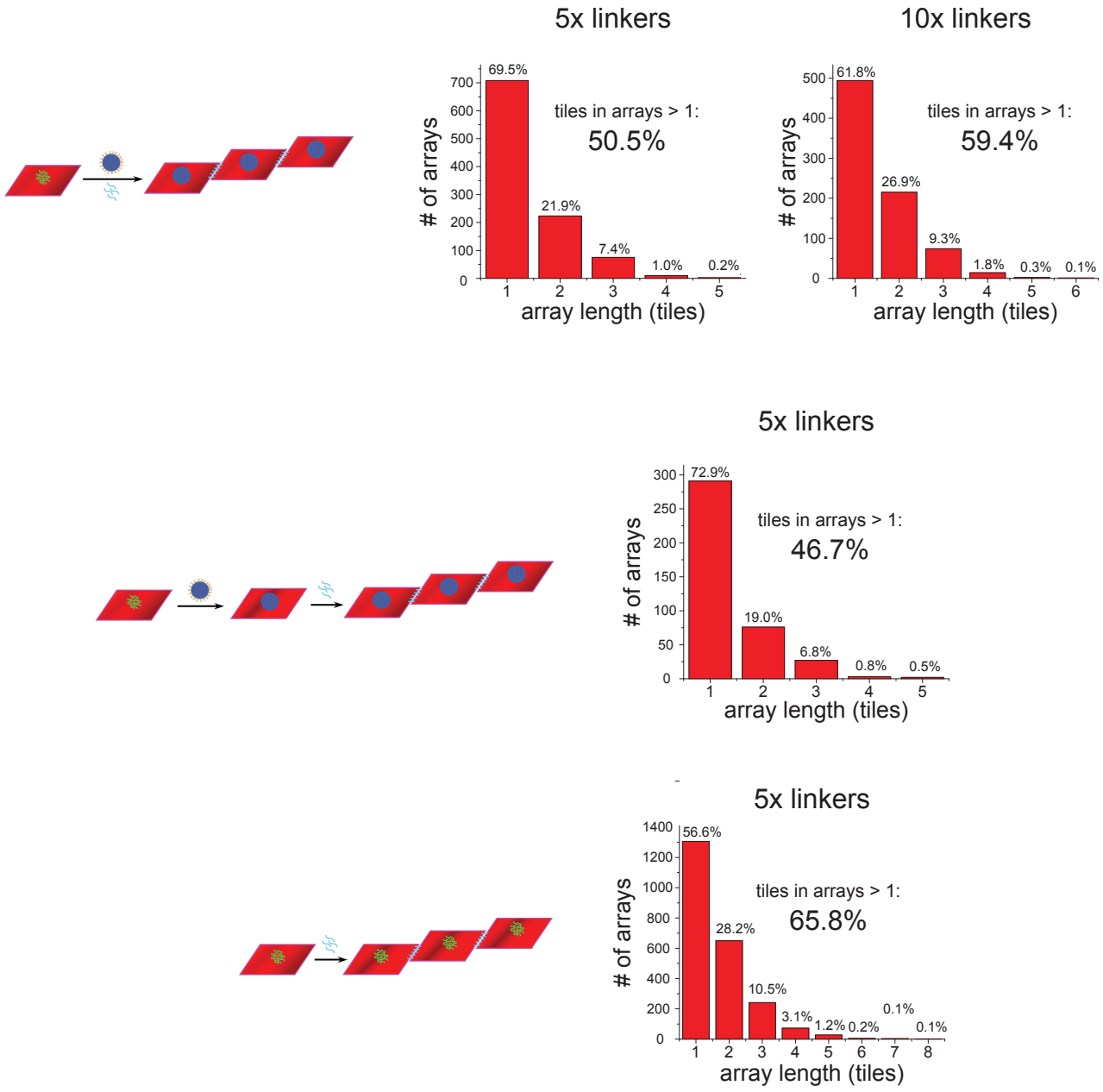

Figure S21. M tile array length distributions. An array length of 1 indicates a single tile not in an array. For the samples that include MS2, virtually complete association of the caspids with tiles was maintained.

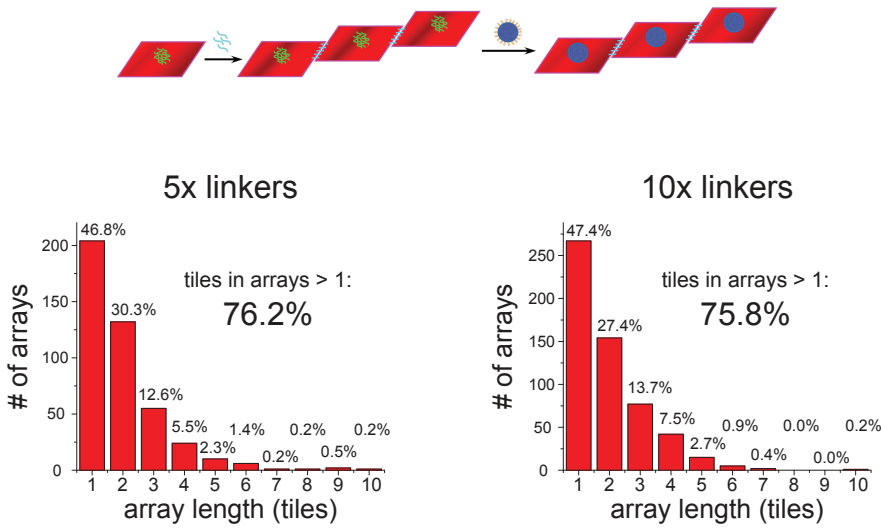

Figure S21 (cont). M tile array length distributions.

Figure S22. DC tile array length distributions. The arrays are counted in the number of capsids in a row, not tiles (as with the E and M tile arrays). An array length of 0 signifies a tile with no capsids bound.

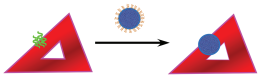

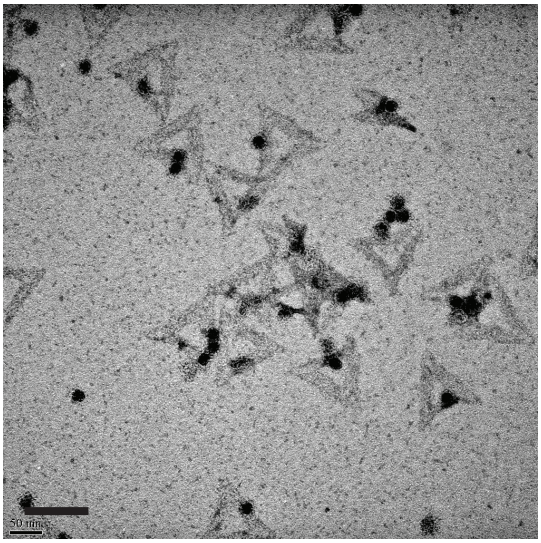

Figure S23. Additional TEM image of Tri1 tiles and MS2. The triangular tiles are clearly visible, as are the caspids adhered to one side. Scale bar: 100 nm.

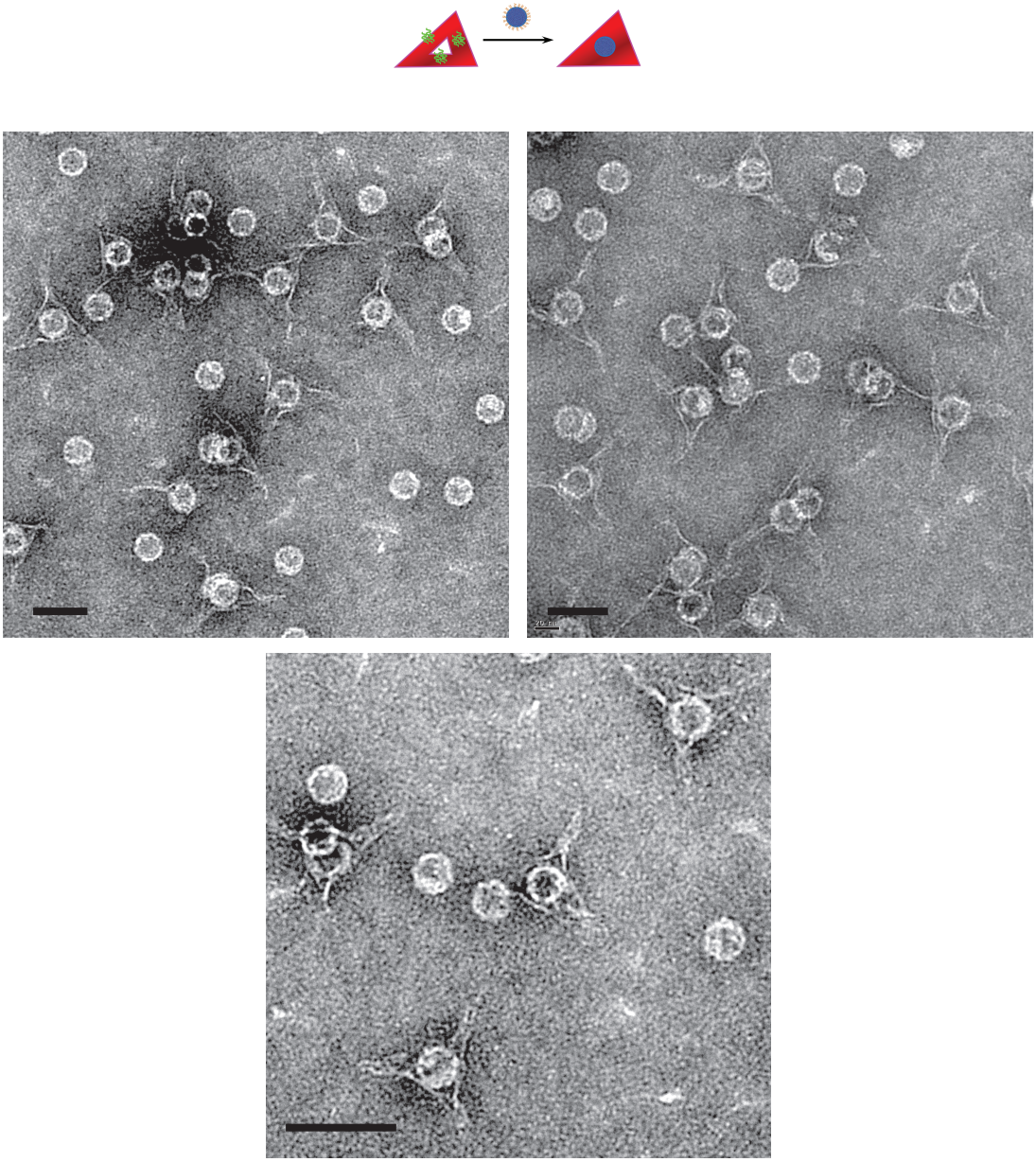

Figure S24. Additional zoom-out TEM images of Tri3 tiles and MS2. The capsids are almost exclusively immobilized in the center of the tiles and pull the three sides inwards towards the center of the tile, distorting them. Scale bars: 50 nm.

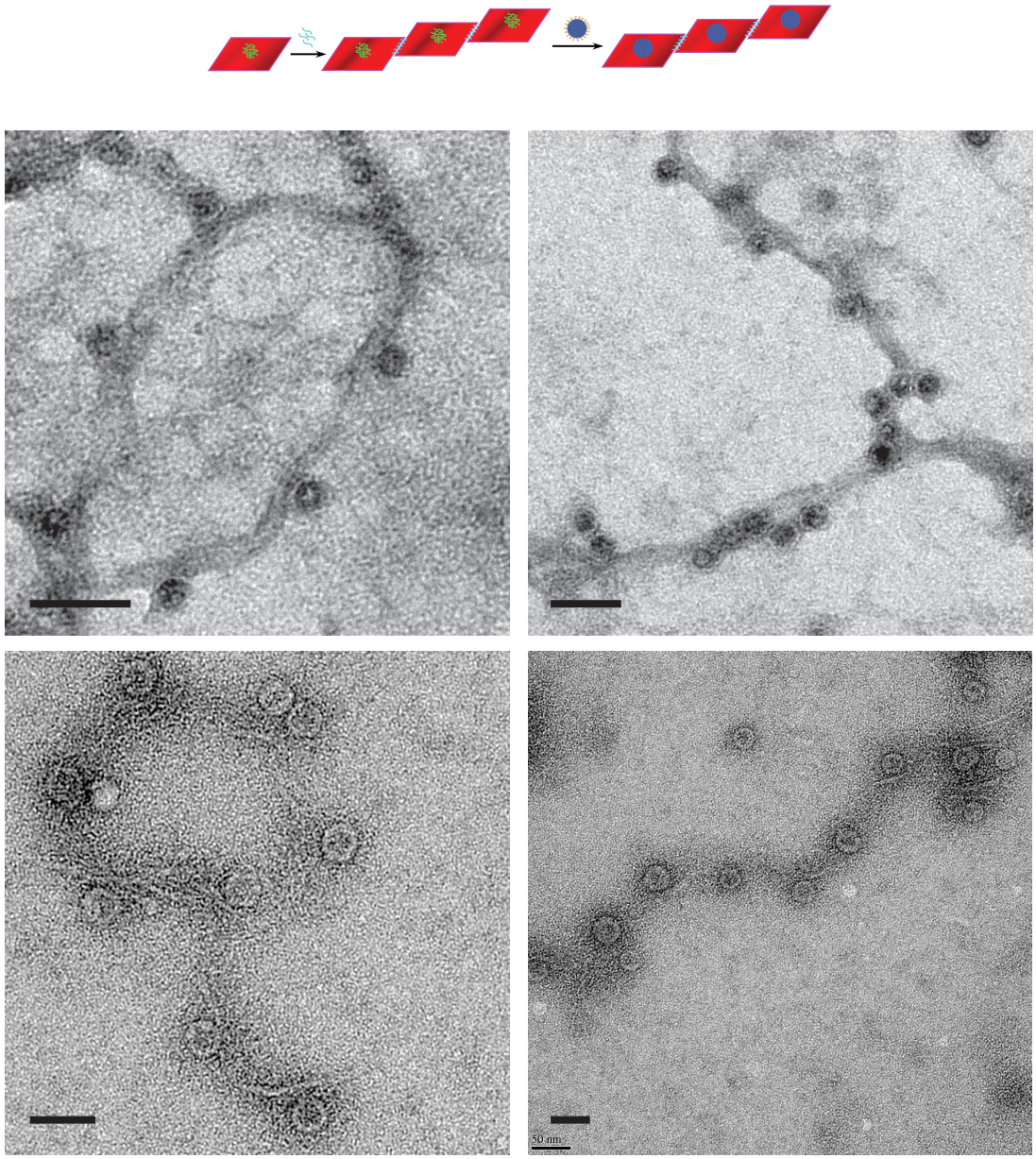

Figure S25. TEM images of M tile arrays with MS2. The tiles do not stain well, and likely shrink due to the uranyl acetate stain, as well as lying sideways on the grid, but the capsids are intact and spaced approximately 100 nm apart. Scale bars: 50 nm.

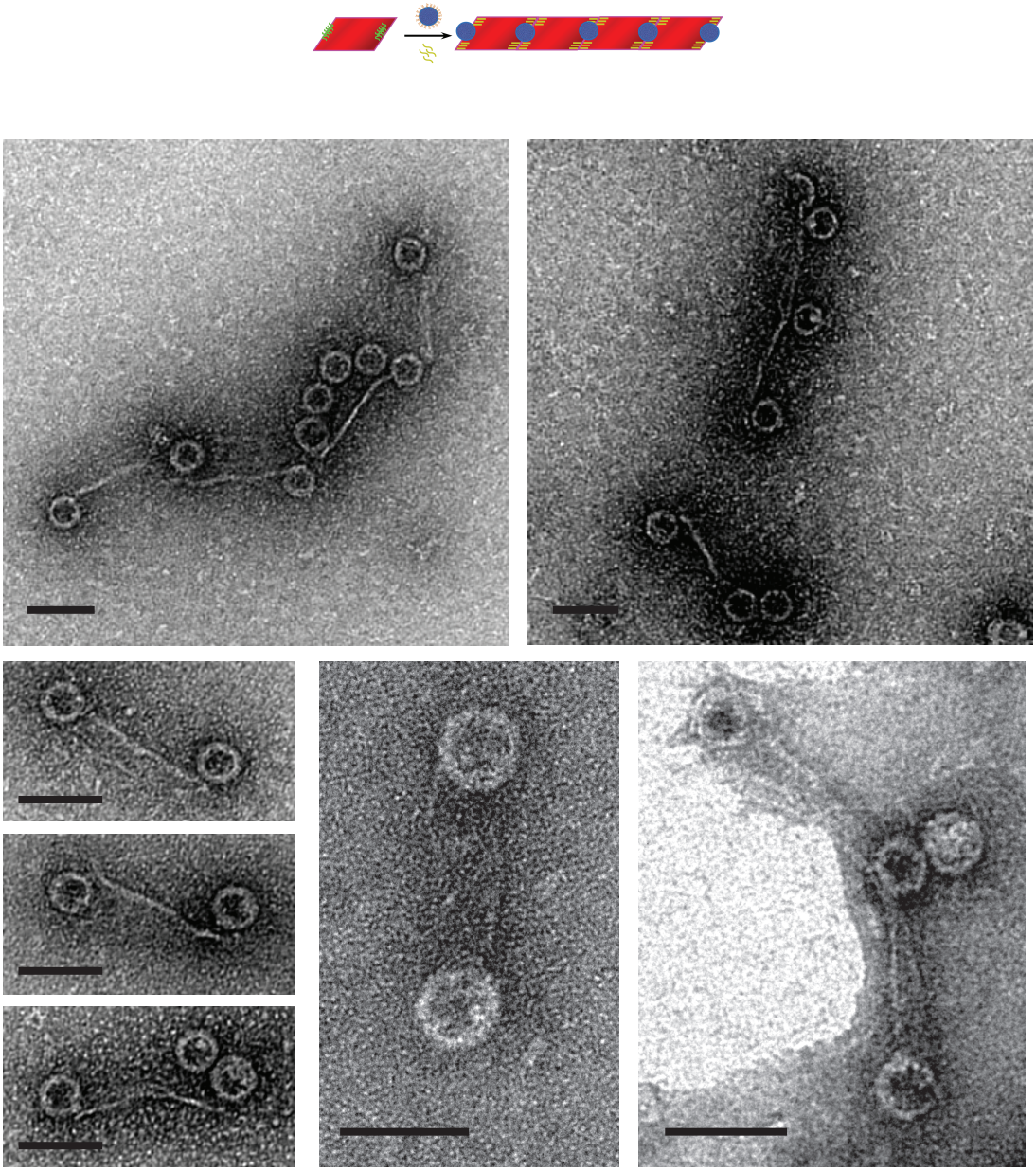

Figure S26. TEM images of DC tile arrays formed with MS2. The arrays most likely adsorb to the grid with the tiles sideways, making them appear as lines connecting the capsids. In addition to illustrating the arrays, these images confirm that the capsids are intact, hollow, and 27 nm in diameter. Scale bars: 50 nm

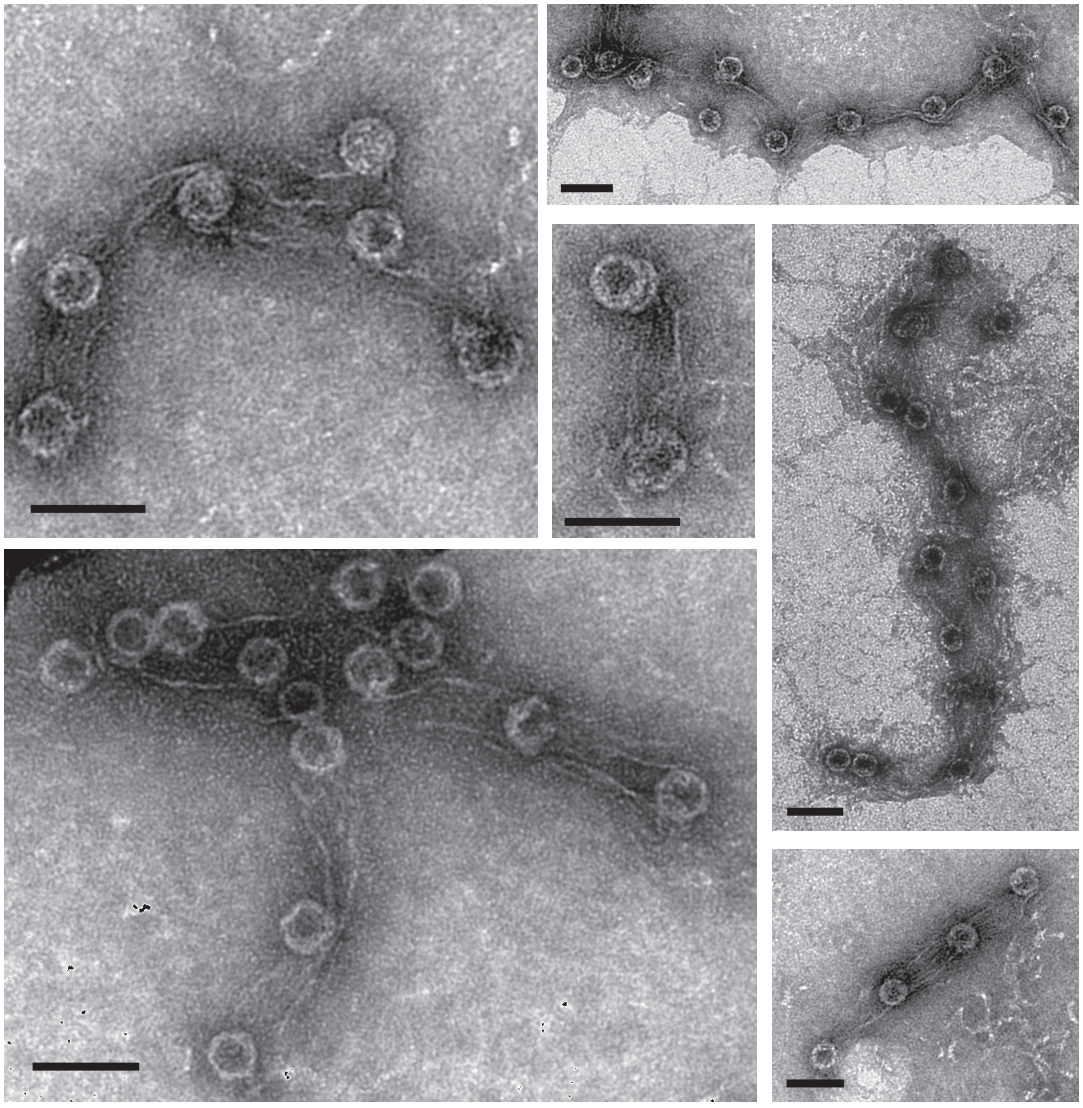

Figure S26 (cont). TEM images of DC tile arrays formed with MS2. Scale bars: 50 nm

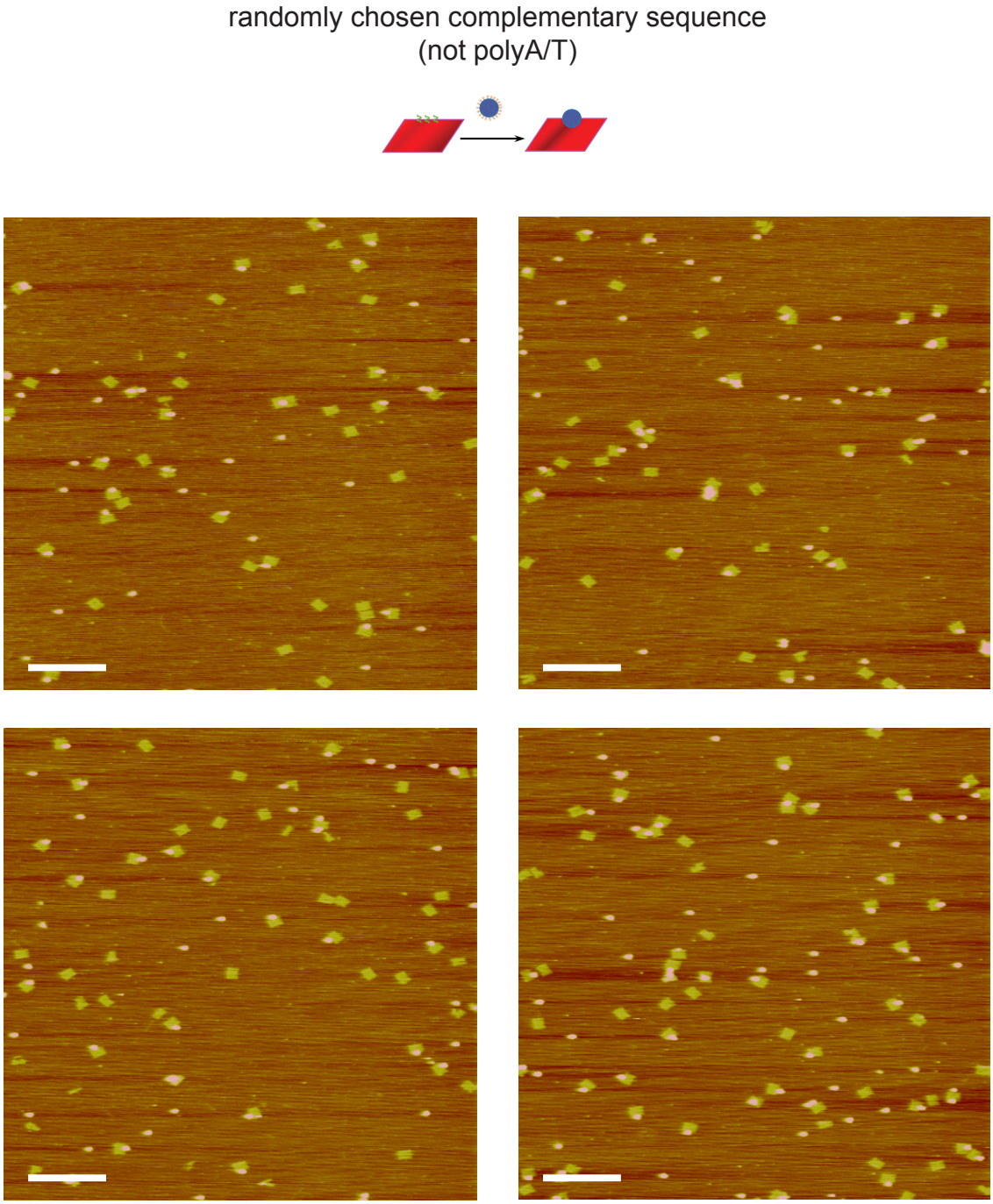

Figure S27. AFM images of capsids and tiles association using a random, complementary sequence (not polyA/T). The probes on the tiles are a random 40-bp sequence and the DNA on the caspids is complementary to the last 20 bp of the probe. The hybridization efficiency does not surpass ~50%, even with